

# AIGV-Assessor: Benchmarking and Evaluating the Perceptual Quality of Text-to-Video Generation with LMM

Jiarui Wang<sup>1</sup>, Huiyu Duan<sup>1,2</sup>, Guangtao Zhai<sup>1,2</sup>, Juntong Wang<sup>1</sup>, Xionghuo Min<sup>1\*</sup>,  
<sup>1</sup>Institute of Image Communication and Network Engineering,  
<sup>2</sup> MoE Key Lab of Artificial Intelligence, AI Institute,  
Shanghai Jiao Tong University, Shanghai, China

## Abstract

*The rapid advancement of large multimodal models (LMMs) has led to the rapid expansion of artificial intelligence generated videos (AIGVs), which highlights the pressing need for effective video quality assessment (VQA) models designed specifically for AIGVs. Current VQA models generally fall short in accurately assessing the perceptual quality of AIGVs due to the presence of unique distortions, such as unrealistic objects, unnatural movements, or inconsistent visual elements. To address this challenge, we first present AIGVQA-DB, a large-scale dataset comprising 36,576 AIGVs generated by 15 advanced text-to-video models using 1,048 diverse prompts. With these AIGVs, a systematic annotation pipeline including scoring and ranking processes is devised, which collects 370k expert ratings to date. Based on AIGVQA-DB, we further introduce AIGV-Assessor, a novel VQA model that leverages spatiotemporal features and LMM frameworks to capture the intricate quality attributes of AIGVs, thereby accurately predicting precise video quality scores and video pair preferences. Through comprehensive experiments on both AIGVQA-DB and existing AIGV databases, AIGV-Assessor demonstrates state-of-the-art performance, significantly surpassing existing scoring or evaluation methods in terms of multiple perceptual quality dimensions. The dataset and code will be released at <https://github.com/wangjiarui153/AIGV-Assessor>.*

## 1. Introduction

Text-to-video generative models [10, 26, 43, 64, 72], including auto-regressive [22, 80] and diffusion-based [10, 26, 55] approaches, have experienced rapid advancements in recent years with the explosion of large multimodal models (LMMs). Given appropriate text prompts, these models can generate high-fidelity and semantically-aligned videos,

commonly referred to as AI-generated videos (AIGVs), which have significantly facilitated the content creation in various domains, including entertainment, art, design, and advertising, etc [38, 78]. Despite the significant progress, current AIGVs are still far from satisfactory. Unlike natural videos, which are usually affected by low-level distortions, such as noise, blur, low-light, etc, AIGVs generally suffer from degradations such as unrealistic objects, unnatural movements, inconsistent visual elements, and misalignment with text descriptions [24, 30, 42, 84].

The unique distortions in AIGVs also bring challenges to the video evaluation. Traditional video quality assessment (VQA) methods [32, 34, 57, 69, 70] mainly focus on evaluating the quality of professionally-generated content (PGC) and user-generated content (UGC), thus struggling to address the specific distortions associated with AIGVs, such as spatial artifacts, temporal inconsistencies, and misalignment between generated content and text prompts. For evaluation of AIGVs, some metrics such as Inception Score (IS) [53] and Fréchet Video Distance (FVD) [61] have been widely used, which are computed over distributions of videos and may not reflect the human preference for an individual video. Moreover, these metrics mainly evaluate the fidelity of videos, while failing to assess the text-video correspondence. Vision-language pre-training models, such as CLIPScore [20], BLIPScore [36], and AestheticScore [54] are frequently employed to evaluate the alignment between generated videos and their text prompts. However, these models mainly consider the text-video alignment at the image level, while ignoring the dynamic diversity and motion consistency of visual elements that are crucial to the video-viewing experience.

In this paper, to facilitate the development of more comprehensive and precise metrics for evaluating AI-generated videos, we present AIGVQA-DB, a large-scale VQA dataset, including 36,576 AIGVs generated by 15 advanced text-to-video models using 1,048 diverse prompts. An overview of the dataset construction pipeline is shown in Figure 1. The prompts are collected from existing

\*Corresponding Author.

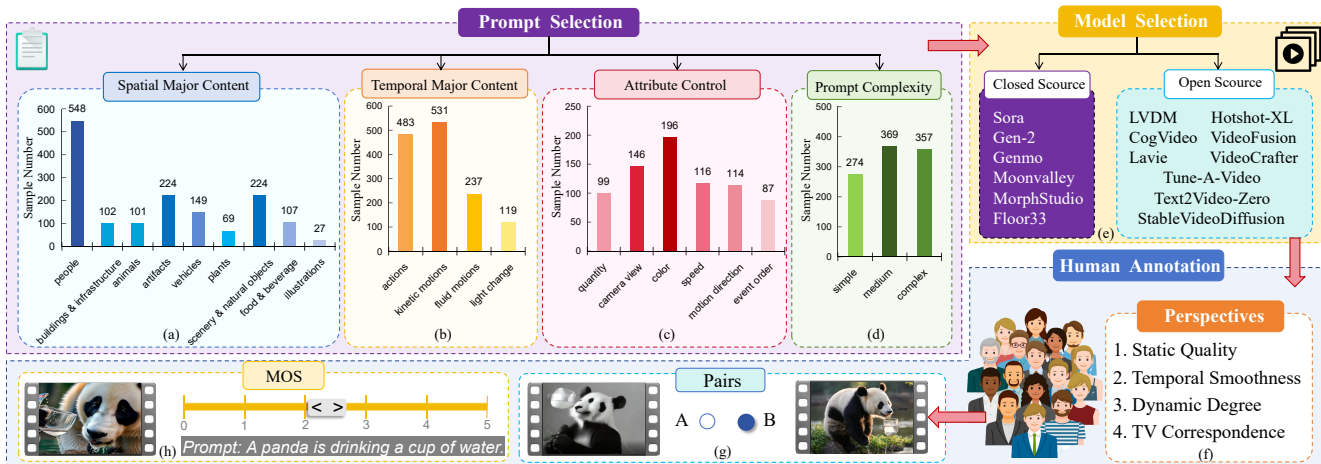


Figure 1. An overview of the AIGVQA-DB construction pipeline, illustrating the generation and the subjective evaluation procedures for the AIGVs in the database. (a) Prompt categorization according to the spatial major content. (b) Prompt categorization according to the temporal descriptions. (c) Prompt categorization according to the attribute control. (d) Prompt categorization according to the prompt complexity. (e) The 15 generative models used in the database. (f) Four visual quality evaluation perspectives, including static quality, temporal smoothness, dynamic degree, and text-video correspondence. (g) and (h) demonstrates the pair comparison and preference scoring processes, respectively.

open-domain text-video datasets [7, 8, 37, 42, 67, 75] or manually-written, which can be categorized based on four orthogonal aspects respectively, as shown in Figure 1(a)-(d). Based on the AIGVs, we collect 370k expert ratings comprising both mean opinion scores (MOSs) and pairwise comparisons, which are evaluated from four dimensions, including: (1) static quality, (2) temporal smoothness, (3) dynamic degree, and (4) text-video correspondence. Equipped with the dataset, we propose **AIGV-Assessor**, a large multimodal model-based (LMM-based) VQA method for AIGVs, which reformulates the quality regression task into an interactive question-and-answer (Q&A) framework and leverages the powerful multimodal representation capabilities of LMMs to provide accurate and robust quality assessments. AIGV-Assessor not only classifies videos into different quality levels through natural language output, but also generates precise quality scores through regression, thus enhancing the interpretability and usability of VQA results. Moreover, AIGV-Assessor also excels in pairwise video comparisons, enabling nuanced assessments that are closer to human preferences. Extensive experimental results demonstrate that AIGV-Assessor outperforms existing text-to-video scoring methods in terms of multiple dimensions relevant to human preference. The main contributions of this paper are summarized as follows:

- We construct AIGVQA-DB, a large-scale dataset comprising 36,576 AI-generated videos annotated with MOS scores and pairwise comparisons. Compared with existing benchmarks, AIGVQA-DB provides a more comprehensive assessment of the capabilities of text-to-video models from multiple perspectives.
- Based on AIGVQA-DB, we evaluate and benchmark 15 representative text-to-video models, and reveal their strengths and weaknesses from four crucial preference di-

Table 1. An overview of popular text-to-video (T2V) and image-to-video (I2V) generation models. <sup>†</sup> Representative variable.

Model	Year	Mode	Resolution	Frames	Open
CogVideo [22]	22.05	T2V	480×480	32	✓
Make-a-Video [55]	22.09	T2V	256×256	16	✓
LVDV [19]	22.11	T2V	256×256	16	✓
Tune-A-Video [72]	22.12	T2V	512×512	8	✓
VideoFusion [43]	23.03	T2V	128×128	16	✓
Text2Video-Zero [26]	23.03	T2V	512×512	8	✓
ModelScope [64]	23.03	T2V	256×256	16	✓
Lavie [66]	23.09	T2V	512×320	16	✓
VideoCrafter [10]	23.10	T2V, I2V	1024×576	16	✓
Hotshot-XL [1]	23.10	T2V	672×384	8	✓
StableVideoDiffusion [9]	23.11	I2V	576×1024	14	✓
AnimateDiff [18]	23.12	T2V, I2V	384×256	20	✓
Floor33 [2]	23.08	T2V, I2V	1024×640	16	–
Genmo [3]	23.10	T2V, I2V	2048×1536	60	–
Gen-2 [4]	23.12	T2V, I2V	1408×768	96	–
MoonValley [5]	24.01	T2V, I2V	1184×672	200 <sup>†</sup>	–
MorphStudio [6]	24.01	T2V, I2V	1920×1080	72	–
Sora [7]	24.02	T2V, I2V	1920×1080	600 <sup>†</sup>	–

mensions, *i.e.*, static quality, temporal smoothness, dynamic degree, and text-to-video correspondence.

- We present a novel LMM-based VQA model for AIGVs, termed AIGV-Assessor, which integrates both spatial and temporal visual features as well as prompt features into a LMM to give quality levels, predict quality scores, and conduct quality comparisons.
- Thorough analysis of our AIGV-Assessor is provided and extensive experiments on our proposed AIGVQA-DB and other AIGV quality assessment datasets have shown the effectiveness and applicability of AIGV-Assessor.

## 2. Related Work

### 2.1. Text-to-video Generation

Recent advancements in text-to-video generative models have substantially broadened video creation and modification possibilities. As shown in Table 1, these models exhibit

Table 2. Summary of existing text-to-image and text-to-video evaluation datasets.

Dataset Types	Name	Numbers	Prompts	Models	Annotators	Dimensions	MOSs / Pairs	Annotation
AIGIQA	AGIQA-3k [33]	2,982	180	6	21	2	5,964	MOS
	AIGCIQA2023 [63]	2,400	100	6	28	3	7,200	MOS
	RichHF-18k [38]	17,760	17,760	3	3	4	71,040	MOS
	HPS [74]	98,807	25,205	1	2,659	1	25,205	Pairs
	Pick-a-Pic [28]	-	37,523	3	4,375	1	584,247	Pairs
AIGVQA	MQT [14]	1,005	201	5	24	2	2,010	MOS
	EvalCrafter [41]	2,500	700	5	7	4	1,024	MOS
	FETV [42]	2,476	619	4	3	3	7,428	MOS
	LGVQ [84]	2,808	468	6	20	3	8,424	MOS
	T2VQA-DB [30]	10,000	1,000	9	27	1	10,000	MOS
	GAIA [11]	9,180	510	18	54	3	27,540	MOS
	<b>AIGVQA-DB(Ours)</b>	<b>36,576</b>	<b>1,048</b>	<b>15</b>	<b>120</b>	<b>4</b>	<b>122,304</b>	<b>MOS and Pairs</b>

distinct characteristics and capacities, including modes, resolution, and total frames. CogVideo [22] is an early text-to-video (T2V) model capable of generating short videos based on CogView2 [15]. Make-a-video [55] adds effective spatial-temporal modules on a diffusion-based text-to-image (T2I) model (*i.e.*, DALLE-2 [51]). VideoFusion [43] also leverages the DALLE-2 and presents a decomposed diffusion process. LVDM [19], Text2Video-Zero [26], Tune-A-Video [72], and ModelScope [64] are models that inherit the success of Stable Diffusion (SD) [52] for video generation. Lavie [66] extends the original transformer block in SD to a spatio-temporal transformer. Hotshot-XL [1] introduces personalized video generation. Beyond these laboratory-driven advancements, the video generation landscape has also been enriched by a series of commercial products. Notable among them are Floor33 [2], Gen-2 [4], Genmo [3], MoonValley [5], MorphStudio [6], and Sora [7], which have gained substantial attention in both academia and industry, demonstrating the widespread application potential of AI-assisted video creation.

## 2.2. Text-to-video Evaluation

The establishment of the AI-generated image quality assessment (AIGIQA) dataset is relatively well-developed, including both mean opinion scores (MOSs) for absolute quality evaluations, and pairwise comparisons for relative quality judgments. Recent developments in text-to-video generation models have also spurred the creation of various AI-generated video quality assessment (AIGVQA) datasets, addressing different aspects of the T2V generation challenge, as shown in Table 2. MQT [14] consists of 1,005 videos generated by 5 models using 201 prompts. EvalCrafter [41] and FETV [42] extend the scale of the videos, prompts, and evaluation dimensions. LGVQ [84] increases the number of annotators, providing more reliable MOSs. T2VQA-DB [30] consists of 10,000 videos from 1,000 prompts representing a significant improvement in scale. GAIA [11] collects 9,180 videos focusing on action quality assessment in AIGVs, but falls short in addressing the consistency between the generated visuals and their textual prompts. Most existing VQA datasets predominantly rely on MOS, an absolute scoring method, which suffers from the same drawback: absolute scores alone may cause ambiguity and overlook subtle quality differences. In contrast,

our AIGVQA-DB includes both MOSs and pairwise comparisons, addressing the limitations of current works by providing fine-grained preference feedbacks.

## 3. Database Construction and Analysis

### 3.1. Data Collection

**Prompt Sources and Categorization.** Prompts of the AIGVQA-DB are primarily sourced from existing open-domain text-video pair datasets, including InternVid [67], MSRVT [75], WebVid [8], TGIF [37], FETV [42] and Sora website [7]. We also manually craft prompts describing highly unusual scenarios to test the generalization ability of the generation models. As shown in Figure 1(a)-(d), we follow the categorization principles from FETV [42] to organize each prompt based on the “spatial major content”, “temporal major content”, “attribute control”, and “prompt complexity”.

**Text-to-Video Generation.** We utilize 15 latest text-to-video generative models to create AI-generated videos as shown in Figure 1(e). We leverage open-source website APIs and code with default weights for these models to produce AIGVs. For the construction of the MOS subset, we collect 48 videos from the Sora Website [7], along with their corresponding text prompts. Using these prompts, we generate additional videos using 11 different generative models. This process results in a total of 576 videos (12 generative models  $\times$  48 prompts). In addition to the MOS subset, we construct the pair-comparison subset using 1,000 diverse prompts, and 12 generative models including 8 open-sourced and 4 close-sourced are employed for text-to-video generation. Specifically, for each prompt, we generate four distinct videos for each open-source generative model and one video for each closed-source generative model. This process yields a total of 36,000 videos. More details of the database can be found in the Appendix B.

### 3.2. Subjective Experiment Setup and Procedure

Due to the unique and unnatural characteristics of AI-generated videos and the varying target video spaces dictated by different text prompts, relying solely on a single score, such as “quality”, to represent human visual preferences is insufficient. In this paper, we propose to measure the human visual preferences of AIGVs from four perspec-

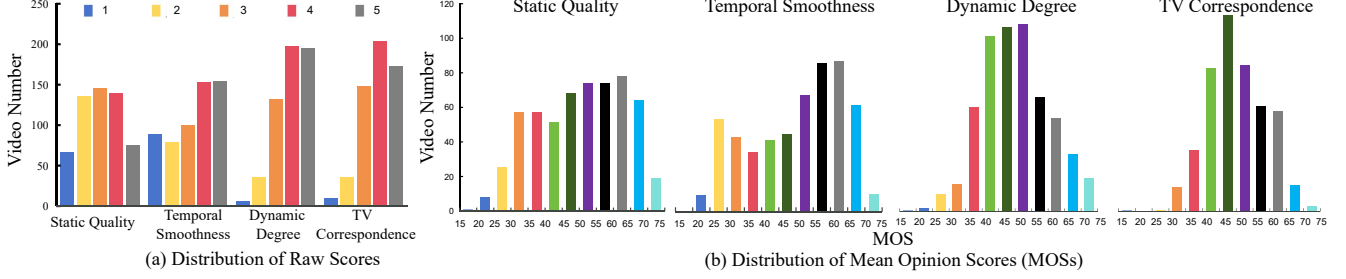


Figure 2. Video score distribution from the four perspectives including static quality, temporal smoothness, dynamic degree, and t2v correspondence. (a) Distribution of raw scores. (b) Distribution of Mean Opinion Scores (MOSs)

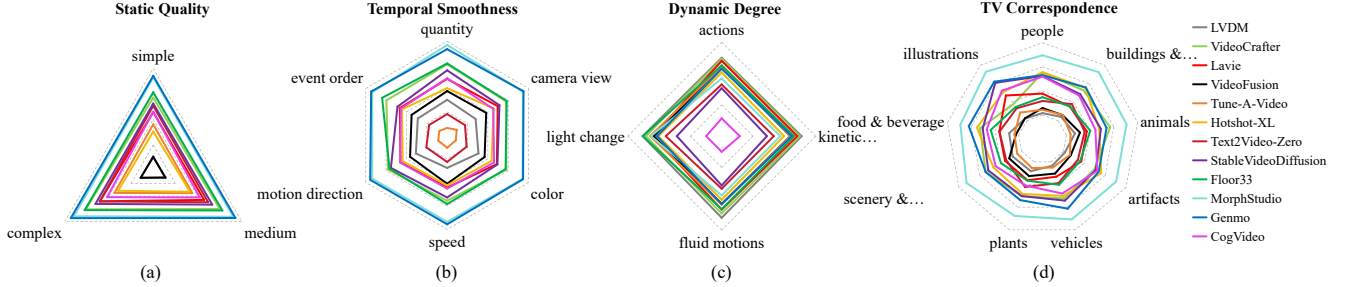


Figure 3. Comparison of averaged win rates of different generation models across different categories. (a) Results across prompt complexity. (b) Results across attribute control. (c) Results across temporal major contents. (d) Results across spatial major contents.

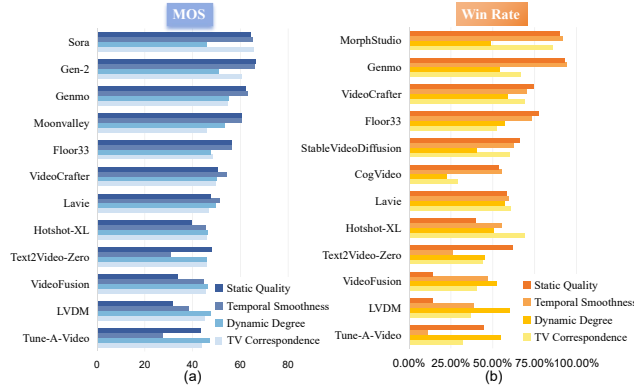


Figure 4. (a) Comparison of text-to-video generation models regarding the MOS in terms of four dimensions sorted bottom-up by their averaged MOS. (b) Comparison of text-to-video generation models regarding the win rate in terms of four dimensions sorted bottom-up by their averaged win rate.

tives. **Static quality** assesses the clarity, sharpness, color accuracy, and overall aesthetic appeal of the frames when viewed as standalone images. **Temporal smoothness** evaluates the temporal coherence of video frames and the absence of temporal artifacts such as flickering or jittering. **Dynamic degree** evaluates the extent to which the video incorporates large motions and dynamic scenes, which contributes to the overall liveliness and engagement measurement of the content. **Text-video (TV) correspondence** assesses how accurately the video content reflects the details, themes, and actions described in the prompt, ensuring that the generated video effectively translates the text input into a visual narrative. Each of these four visual perception

perspectives is related but distinct, offering a comprehensive evaluation for AIGVs. To evaluate the quality of the videos in the AIGVQA-DB, we conduct subjective experiments adhering to the guidelines outlined in ITU-R BT.500-14 [16]. For the MOS annotation type, we use a 1-5 Likert-scale judgment to score the videos. For the pairs annotation type, participants are presented with pairs of videos and asked to choose the one they prefer, providing a direct comparison method for evaluating relative video quality. The videos are displayed using an interface designed with Python Tkinter, as illustrated in Figure 1(g)-(h). A total of 120 graduate students participate in the experiment.

### 3.3. Subjective Data Processing

In order to obtain the MOS for an AIGV, we linearly scale the raw ratings to the range [0, 100] as follows:

$$z_{ij} = \frac{r_{ij} - \mu_{ij}}{\sigma_i}, \quad z'_{ij} = \frac{100(z_{ij} + 3)}{6},$$

$$\mu_i = \frac{1}{N_i} \sum_{j=1}^{N_i} r_{ij}, \quad \sigma_i = \sqrt{\frac{1}{N_i - 1} \sum_{j=1}^{N_i} (r_{ij} - \mu_{ij})^2}$$

where  $r_{ij}$  is the raw ratings given by the  $i$ -th subject to the  $j$ -th video.  $N_i$  is the number of videos judged by subject  $i$ . Next, the MOS of the video  $j$  is computed by averaging the rescaled z-scores as follows:

$$MOS_j = \frac{1}{M} \sum_{i=1}^M z'_{ij}$$

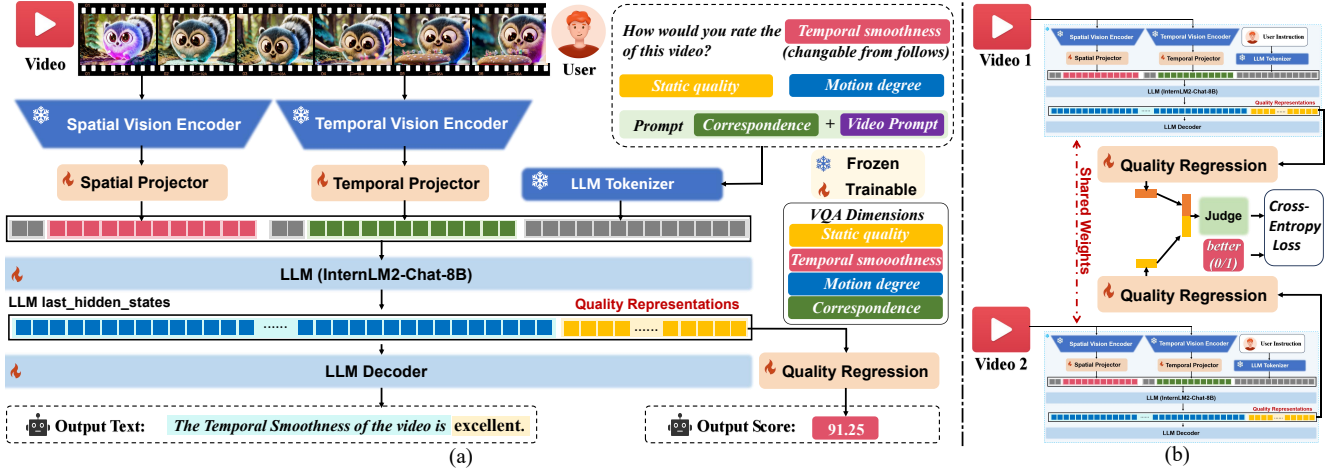


Figure 5. The framework of AIGV-Assessor: (a) AIGV-Assessor takes AI-generated video frames as input and outputs both text-based quality levels and numerical quality scores. The system begins with the extraction of spatiotemporal features using two vision encoders, which are then passed through spatial and temporal projection modules to generate aligned visual tokens into language space. The LLM decoder produces text-based feedback describing the video quality level for four evaluation dimensions, respectively. Simultaneously, the last-hidden-states from the LLM are used to perform quality regression that outputs final quality scores in terms of four dimensions. (b) AIGV-Assessor is fine-tuned on pairwise comparison, further allowing the model to output the evaluation comparison between two videos.

where  $MOS_j$  indicates the MOS for the  $j$ -th AIGV,  $M$  is the number of subjects, and  $z'_{ij}$  are the rescaled z-scores.

For the pairs annotation type, given a text prompt  $p_i$ , and 12 video generation models labeled  $\{A, B, C, \dots, L\}$ , we generate videos using each model, forming a group of videos  $G_{i,j} = \{V_{i,A,j}, V_{i,B,j}, V_{i,C,j}, \dots, V_{i,L,j}\}$ . For each prompt  $p_i$ , we generate four different videos randomly for each of the eight open-source generative models and one video for each of the four closed-source generative models, resulting in a group of 36 videos  $\{G_{i,A,1}, G_{i,A,2}, G_{i,A,3}, G_{i,A,4}, G_{i,B,1}, \dots, G_{i,L,1}\}$ . For each group, we create all possible pairwise combinations, resulting in  $C_{36}^2$  pairs:  $(V_{A1}, V_{B1}), (V_{A1}, V_{B2}), (V_{A1}, V_{B3}), (V_{A1}, V_{B4}), (V_{A1}, V_{C1}), \dots, (V_{K1}, V_{L1})$ . In the AIGVQA-DB construction pipeline, a prompt suite of 1000 prompts results in 630,000 ( $1000 \times C_{36}^2$ ) pairwise video comparisons. From this extensive dataset, we randomly sample 30,000 pairs for evaluation from four perspectives. Each pair is judged by three annotators, and the final decision of the better video in each pair is determined by the majority vote. Finally, we obtain a total of 46,080 reliable score ratings (20 annotators  $\times$  4 perspectives  $\times$  576 videos) and 360,000 pair ratings (3 annotators  $\times$  4 perspectives  $\times$  30,000 pairs).

### 3.4. AIGV Analysis from Four Perspectives

As shown in Figure 2, the videos in the AIGVQA-DB cover a wide range of perceptual quality. We further analyze the win rates of various generation models across categories in Figure 3, revealing the strengths and weaknesses of each T2V model. As shown in Figure 3(a), the performances of T2V models rank uniform for different prompt complexity items in terms of static quality, which manifests current T2V model rank consistently for different prompts, likely

due to shared architectures like diffusion-based systems, with common strengths and limitations in handling complex prompts. As shown in Figure 3(b), in terms of attribute control, StableVideoDiffusion [9] excels in managing quantity over event order, as it first generates static images before animating them, preserving the original event sequence. As shown in Figure 3(d), in terms of spatial content, most videos featuring “plants” and “people” show poor T2V correspondence. More comparison and analysis can be found in the Appendix D. We also launch comparisons among text-to-video generation models regarding the MOS and pairwise win rates shown in Figure 4. Notably, models such as LVDM [19] demonstrate exceptional performance in handling dynamic content, but exhibit relatively lower performance in temporal smoothness. Sora [7] and MorphStudio [6] perform well in static quality and temporal smoothness while lagging in dynamic degree. Additionally, closed-source models exhibit much better performance compared to open-source models.

## 4. Proposed Method

### 4.1. Model Structure

**Spatial and Temporal Vision Encoder.** As shown in Figure 5(a), the model leverages two different types of encoders to capture the spatial and temporal characteristics of the video: (1) 2D Encoder: A pre-trained 2D vision transformer (InternViT [68]) is used to process individual video frames. (2) 3D Encoder: A 3D network, *i.e.*, SlowFast [17], is employed to extract temporal features by processing sequences of video frames.

**Spatiotemporal Projection Module.** Once the spatial and temporal features are extracted, they are projected into a

Table 3. Performance comparisons of the state-of-the-art quality evaluation methods on the AIGVQA-DB from four perspectives. The best performance results are marked in **RED** and the second-best performance results are marked in **BLUE**.

Dimension	Static Quality				Temporal Smoothness				Dynamic Degree				TV Correspondence			
	Methods / Metrics	Pair Acc	SRCC	PLCC	KRCC	Pair Acc	SRCC	PLCC	KRCC	Pair Acc	SRCC	PLCC	KRCC	Pair Acc	SRCC	PLCC
NIQE [48]	54.32%	0.0867	0.1626	0.0615	52.67%	0.0641	0.1152	0.0451	45.64%	0.1765	0.2448	0.1194	46.99%	0.1771	0.2231	0.1193
QAC [79]	49.96%	0.1022	0.1363	0.0680	54.90%	0.1633	0.2039	0.1105	54.72%	0.0448	0.0427	0.0295	54.48%	0.0303	0.0197	0.2233
BRISQUE [47]	59.98%	0.2909	0.2443	0.1969	55.67%	0.2325	0.1569	0.1553	44.60%	0.1351	0.0959	0.0893	51.02%	0.1294	0.1017	0.0869
BPRI [45]	52.28%	0.2181	0.1723	0.1398	47.26%	0.1766	0.0880	0.1138	46.83%	0.1956	0.1688	0.1329	49.13%	0.1569	0.1548	0.1052
HOSA [76]	61.54%	0.2420	0.2106	0.1643	57.31%	0.2311	0.1757	0.1559	44.97%	0.0755	0.0449	0.0496	52.23%	0.1645	0.1324	0.1097
BMPRI [46]	53.71%	0.1690	0.1481	0.1075	49.31%	0.1434	0.0844	0.0894	45.07%	0.1153	0.0925	0.0777	48.43%	0.1567	0.1500	0.1041
V-Dynamic [24]	51.34%	0.0768	0.0792	0.0494	31.91%	0.3713	0.4871	0.2557	53.11%	0.1466	0.0253	0.0988	46.96%	0.0405	0.0576	0.0223
V-Smoothness [24]	61.63%	0.6748	0.4506	0.4590	76.59%	0.8526	0.8313	0.6533	47.63%	0.2446	0.2328	0.1580	61.28%	0.3188	0.3073	0.2214
CLIPScore [20]	47.09%	0.0731	0.0816	0.0473	46.33%	0.0423	0.0334	0.0271	52.99%	0.0675	0.0835	0.0439	55.62%	0.1519	0.1731	0.1014
BLIPScore [36]	53.24%	0.0492	0.0421	0.0330	53.07%	0.0659	0.0487	0.0437	53.03%	0.1786	0.1904	0.1205	61.53%	0.1813	0.1896	0.1219
AestheticScore [54]	70.24%	0.6713	0.6959	0.4784	54.82%	0.5154	0.4946	0.3484	52.96%	0.2295	0.2322	0.1527	59.64%	0.2381	0.2440	0.1602
ImageReward [77]	56.69%	0.2606	0.2646	0.1749	54.09%	0.2382	0.2305	0.1600	53.90%	0.1840	0.1836	0.1237	63.97%	0.2311	0.2450	0.1568
UMTScore [42]	48.93%	0.0168	0.0199	0.0117	49.93%	0.0302	0.0370	0.0207	52.69%	0.0168	0.0198	0.0117	53.82%	0.0172	0.0065	0.0108
Video-LLaVA [39]	50.90%	0.0384	0.0513	0.0297	50.36%	0.0431	0.0281	0.0347	50.34%	0.1561	0.1436	0.1176	50.54%	0.1364	0.1051	0.1009
Video-ChatGPT [44]	51.20%	0.1242	0.1587	0.0940	50.16%	0.0580	0.0533	0.0453	50.47%	0.0724	0.0436	0.0563	50.07%	0.0357	0.0124	0.0274
LLaVA-NeXT [35]	52.85%	0.1239	0.1625	0.0954	52.41%	0.4021	0.3722	0.3052	51.84%	0.1767	0.1655	0.1328	59.20%	0.4116	0.3428	0.3261
VideoLLaMA2 [12]	52.73%	0.2643	0.3271	0.1928	52.27%	0.3608	0.2450	0.2696	50.78%	0.1900	0.1561	0.1379	54.25%	0.1656	0.1633	0.1210
Qwen2-VL [65]	56.50%	0.4922	0.5291	0.3838	49.12%	0.1681	0.4219	0.1233	52.08%	0.1122	0.1335	0.0849	53.30%	0.3111	0.2775	0.2306
HyperIQA [56]	68.30%	0.7931	0.8093	0.5969	54.65%	0.7426	0.6630	0.5407	53.32%	0.2103	0.2100	0.1384	57.54%	0.6226	0.6250	0.4432
MUSIQ [25]	66.46%	0.7880	0.8044	0.5773	55.16%	0.7199	0.6920	0.5034	52.85%	0.5206	0.4846	0.3521	58.46%	0.4125	0.4093	0.2844
LIQE [83]	63.86%	0.8776	0.8691	0.7008	55.84%	0.7935	0.7720	0.6084	49.02%	0.5303	0.5840	0.3837	55.10%	0.3862	0.3639	0.2640
VSFA [34]	46.43%	0.3365	0.3421	0.2268	50.95%	0.3317	0.3273	0.2202	51.46%	0.1201	0.1362	0.0815	48.07%	0.1024	0.1064	0.0666
BVQA [32]	29.98%	0.4594	0.4701	0.3268	37.65%	0.3704	0.3819	0.2507	<b>55.08%</b>	0.4594	0.4701	0.3268	42.32%	0.3720	0.3978	0.2559
simpleVQA [57]	68.12%	0.8355	0.6438	0.8489	54.14%	0.7082	0.7008	0.4978	53.08%	0.4671	0.3160	<b>0.3994</b>	58.20%	0.4643	0.5440	0.3163
FAST-VQA [69]	70.64%	0.8738	0.8644	0.6860	<b>62.93%</b>	0.9036	0.9134	0.7166	54.34%	0.5603	<b>0.5703</b>	0.3895	<b>65.05%</b>	<b>0.6875</b>	<b>0.6704</b>	<b>0.4978</b>
DOVER [70]	<b>72.92%</b>	<b>0.8907</b>	<b>0.8895</b>	<b>0.7004</b>	58.83%	<b>0.9063</b>	<b>0.9195</b>	<b>0.7187</b>	53.16%	0.5549	0.5489	0.3800	62.35%	0.6783	0.6802	0.4969
Q-Align [71]	71.86%	0.8516	0.8383	0.6641	57.95%	0.8116	0.7025	0.6195	53.71%	<b>0.5655</b>	0.5012	0.3950	62.91%	0.5542	0.5647	0.3870
Ours	<b>79.83%</b>	<b>0.9162</b>	<b>0.9190</b>	<b>0.7576</b>	<b>76.60%</b>	<b>0.9232</b>	<b>0.9216</b>	<b>0.8038</b>	<b>60.30%</b>	<b>0.6093</b>	<b>0.6082</b>	<b>0.4435</b>	<b>70.32%</b>	<b>0.7500</b>	<b>0.7697</b>	<b>0.5591</b>
Improvement	+6.9%	+2.7%	+3.0%	+5.7%	13.7%	+1.7%	+0.2%	+8.5%	+5.2%	+4.4%	+3.8%	+4.4%	+5.3%	+6.3%	+9.9%	+6.13%

shared feature space for alignment with text-based queries. This is done through two projection modules that map the spatial and temporal visual features respectively into the language space. The mapped visual tokens are aligned with text tokens, enabling the model to query the video content in a multimodal fashion.

**Feature Fusion and Quality Regression.** We apply LLM (InternVL2-8B [68]) to combine the visual tokens and user-provided quality prompts to perform the following tasks: (1) Quality level descriptions: the model generates a descriptive quality level evaluation of the input video, such as “The static quality of the video is (bad, poor, fair, good, excellent).” This initial categorization provides a preliminary classification of the video’s quality, which is beneficial for subsequent quality regression tasks. By obtaining a rough quality level, the model can more accurately predict numerical scores in later evaluations. (2) Regression score output: the model uses the final hidden states from the LLM to perform a regression task, outputting numerical quality scores for the video from four different dimensions.

## 4.2. Training and Fine-tuning Strategy

The training process of AIGV-Assessor follows a three-stage approach to ensure high-quality video assessment with quality level prediction, individual quality scoring, and pairwise preference comparison capabilities. This process includes: (1) training the spatial and temporal projectors to align visual and language features, (2) fine-tuning the vision

encoder and LLM with LoRA [23], and training the quality regression module to generate accurate quality scores, (3) incorporating pairwise comparison training using the pairwise comparison subset with a pairwise loss function for robust video quality comparison.

**Spatiotemporal Projector Training.** The first stage focuses on training the spatial and temporal projectors to extract meaningful spatiotemporal visual features and map them into the language space. Through this process, the LLM is able to produce the quality level descriptions *i.e.*, bad, poor, fair, good, excellent.

**Quality Regression Fine-tuning.** Once the model can generate coherent descriptions of video quality level, the second stage focuses on fine-tuning the quality regression module. The goal here is to enable the model to output stable and precise numerical quality scores (MOS-like predictions). The quality regression model takes the last-hidden-state features from LLM as input and generates quality scores from four perspectives. The training objective uses an L1 loss function to minimize the difference between the predicted quality score and the groundtruth MOS.

**Pairwise Comparison Fine-tuning.** The third stage mainly focuses on integrating the pairwise comparison into the training pipeline. As shown in Figure 5(b), two input video pairs share network weights within the same batch. We design a judge network inspired by LPIPS [81] to determine which video performs better. This network leverages

Table 4. Performance comparisons on LGVQ [84] and FETV [42].

Aspects	Methods	LGVQ			FETV		
		SRCC	PLCC	KRCC	SRCC	PLCC	KRCC
Spatial	MUSIQ [25]	0.669	0.682	0.491	0.722	0.758	0.613
	StairIQA [59]	0.701	0.737	0.521	0.806	0.812	0.643
	CLIP-IQA [62]	0.684	0.709	0.502	0.741	0.767	0.619
	LIQE [83]	0.721	0.752	0.538	0.765	0.799	0.635
	UGVQ [84]	<b>0.759</b>	<b>0.795</b>	<b>0.567</b>	<b>0.841</b>	<b>0.841</b>	<b>0.685</b>
	<b>Ours</b>	<b>0.803</b>	<b>0.819</b>	<b>0.617</b>	<b>0.853</b>	<b>0.856</b>	<b>0.699</b>
	<i>Improvement</i>	+4.4%	+2.4%	+5.0%	+1.2%	+1.5%	+1.4%
Temporal	VSFA [34]	0.841	0.857	0.643	0.839	0.859	0.705
	SimpleVQA [57]	0.857	0.867	0.659	0.852	0.862	0.726
	FastVQA [69]	0.849	0.843	0.647	0.842	0.847	0.714
	DOVER [70]	0.867	0.878	0.672	0.868	0.881	0.731
	UGVQ [84]	<b>0.893</b>	<b>0.907</b>	<b>0.703</b>	<b>0.897</b>	<b>0.907</b>	<b>0.753</b>
	<b>Ours</b>	<b>0.900</b>	<b>0.920</b>	<b>0.717</b>	<b>0.936</b>	<b>0.940</b>	<b>0.815</b>
	<i>Improvement</i>	+0.7%	+1.3%	+1.4%	+3.9%	+3.3%	+6.2%
Alignment	CLIPScore [20]	0.446	0.453	0.301	0.607	0.633	0.498
	BLIPScore [36]	0.455	0.464	0.319	0.616	0.645	0.505
	ImageReward [77]	0.498	0.499	0.344	0.657	0.687	0.519
	PickScore [27]	0.501	0.515	0.353	0.669	0.708	0.533
	HPSv2 [73]	0.504	0.511	0.357	0.686	0.703	0.540
	UGVQ [84]	<b>0.551</b>	<b>0.555</b>	<b>0.394</b>	<b>0.734</b>	<b>0.737</b>	<b>0.572</b>
<b>Ours</b>	<b>0.577</b>	<b>0.578</b>	<b>0.411</b>	<b>0.753</b>	<b>0.746</b>	<b>0.585</b>	
	<i>Improvement</i>	+2.6%	+2.3%	+1.7%	+1.9%	+0.9%	+1.3%

learned features and evaluates the perceptual differences between the two videos, allowing more reliable quality assessments in video pair comparison.

**Loss Function.** In the first stage, the spatial and temporal projectors are trained to align visual and language features using language loss. The second stage refines the vision encoder, LLM, and quality regression module’s scoring ability with an L1 loss. The third stage incorporates pairwise comparison training with cross-entropy loss to improve the model’s performance on relative quality evaluation.

## 5. Experiments

### 5.1. Experiment Settings

**Evaluation Datasets and Metrics.** Our proposed method is validated on five AIGVQA datasets: AIGVQA-DB, LGVQ [84], FETV [42], T2VQA [30], and GAIA [11]. To evaluate the correlation between the predicted scores and the ground-truth MOSs, we utilize three evaluation criteria: Spearman Rank Correlation Coefficient (SRCC), Pearson Linear Correlation Coefficient (PLCC), and Kendall’s Rank Correlation Coefficient (KRCC). For pair comparison, we adopt the comparison accuracy as the metric.

**Reference Algorithms.** To assess the performance of our proposed method, we select state-of-the-art evaluation metrics for comparison, which can be classified into five groups: (1) Handcrafted-based I/VQA models, including: NIQE [48], BRISQUE [47], QAC [79], BMPRI [46], HOSA [76], BPRI [45], HIGRADE [31], *etc.* (2) Action-related evaluation models, including: V-Dynamic [24], V-Smoothness [24] which are proposed in VBench [24]. (3) Vision-language pre-training models, including: CLIPScore [20], BLIPScore [36], AestheticScore [54], ImageReward [77], and UMTScore [42]. (4) LLM-based models, in-

Table 5. Performance comparisons on T2VQA-DB [30].

Aspects	Methods	T2VQA-DB			Sora Testing		
		SRCC	PLCC	KRCC	SRCC	PLCC	KRCC
zero-shot	CLIPScore [20]	0.1047	0.1277	0.0702	0.2116	0.1538	0.1406
	BLIPScore [36]	0.1659	0.1860	0.1112	0.2116	0.1038	0.1515
	ImageReward [77]	0.1875	0.2121	0.1266	0.0992	0.0415	0.0748
	UMTScore [42]	0.0676	0.0721	0.0453	0.2594	0.0840	0.1680
finetuned	SimpleVQA [57]	0.6275	0.6388	0.4466	0.0340	0.2344	0.0237
	BVQA [36]	0.7390	0.7486	0.5487	0.4235	0.2489	0.2635
	FAST-VQA [69]	0.7173	0.7295	0.5303	0.4301	0.2369	0.2939
	DOVER [70]	0.7609	0.7693	0.5704	0.4421	0.2689	0.2757
	T2VQA [30]	<b>0.7965</b>	<b>0.8066</b>	<b>0.6058</b>	<b>0.6485</b>	<b>0.3124</b>	<b>0.4874</b>
	<b>Ours</b>	<b>0.8131</b>	<b>0.8222</b>	<b>0.6364</b>	<b>0.6612</b>	<b>0.3318</b>	<b>0.5075</b>
	<i>Improvement</i>	+1.7%	+1.6%	+3.1%	+1.3%	+1.9%	+2.0%

Table 6. Performance comparisons on GAIA [11].

Dimension	Methods / Metrics	Subject		Completeness		Interaction	
		SRCC	PLCC	SRCC	PLCC	SRCC	PLCC
V-Smoothness [24]		0.2402	0.1913	0.1474	0.1625	0.1741	0.1693
V-Dynamic [24]		0.1285	0.0831	0.0903	0.0682	0.1141	0.0758
Action-Score [41]		0.2023	0.1823	0.2867	0.2623	0.2689	0.2432
Flow-Score [41]		0.1471	0.1541	0.0816	0.1273	0.1041	0.1309
CLIPScore [20]		0.3398	0.3330	0.3944	0.3871	0.3875	0.3821
BLIPScore [36]		0.3453	0.3386	0.4174	0.4082	0.4044	0.3994
LLaVAScore [40]		0.3484	0.3436	0.4189	0.4133	0.4077	0.4025
TLVQM [29]		0.5037	0.5137	0.4127	0.4158	0.4079	0.4093
VIDEVAL [60]		0.5237	0.5446	0.4283	0.4375	0.4121	0.4234
VSFA [34]		0.5594	0.5762	0.4940	0.5017	0.4709	0.4811
BVQA [36]		0.5702	0.5888	0.4876	0.4946	0.4761	0.4825
SimpleVQA [58]		0.5920	0.5974	0.4981	0.5078	0.4843	0.4971
FAST-VQA [69]		0.6015	0.6092	0.5157	0.5215	0.5154	0.5216
DOVER [70]		<b>0.6173</b>	<b>0.6301</b>	<b>0.5198</b>	<b>0.5323</b>	<b>0.5164</b>	<b>0.5278</b>
<b>Ours</b>		<b>0.6842</b>	<b>0.6897</b>	<b>0.6635</b>	<b>0.6694</b>	<b>0.6329</b>	<b>0.6340</b>
	<i>Improvement</i>	+6.7%	+6.0%	+14.4%	+13.7%	+11.65%	+10.6%

cluding: Video-LLaVA [39], Video-ChatGPT [44], LLaVA-NeXT [35], VideoLLaMA2 [12], and Qwen2-VL [65]. (5) Deep learning-based I/VQA models, including: HyperIQA [56], MUSIQ [25], LIQE [83], VSFA [34], BVQA [32], SimpleVQA [58], FAST-VQA [69], DOVER [70], and Q-Align [71].

**Training Settings.** Traditional handcrafted models are directly evaluated on the corresponding databases, and the average score of all frames is calculated. For vision-language pre-training and LLM-based models, we load the pre-trained weights for inference. CLIPScore [20], BLIPScore [36], and other vision-language pre-training models are calculated directly as the average cosine similarity between text and each video frame. SimpleVQA [58], BVQA [32], FAST-VQA [69], DOVER [70], and Q-Align [71] are fine-tuned on every test dataset. For deep learning-based IQA and VQA models, all experiments for each method are retrained on each dimension using the same training and testing split as the previous literature at a ratio of 4:1. All results are averaged after ten random splits.

### 5.2. Results and Analysis

Table 3 presents the pairwise win rates and the score prediction correlation between predicted results and human ground truths. The results indicate that handcrafted-based methods consistently underperform across all four evalu-

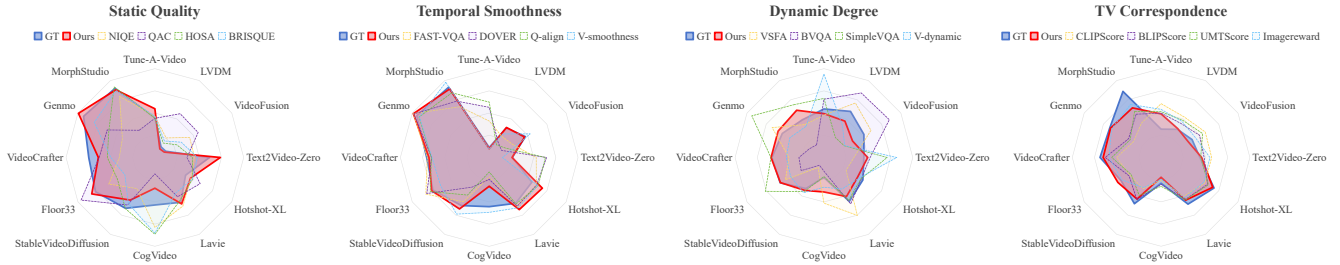


Figure 6. Comparison of win rates of different generation models across four dimensions evaluated by different VQA methods, demonstrating our AIGV-Assessor has better win-rate evaluation ability aligned with Ground Truth (GT).

Table 7. Ablation study of the proposed AIGV-Assessor method.

No.	Feature & Strategy				Static Quality			Temporal Smoothness			Dynamic Degree			T2V Correspondence		
	spatial	temporal	quality level	LoRA finetuning	SRCC	PLCC	KRCC	SRCC	PLCC	KRCC	SRCC	PLCC	KRCC	SRCC	PLCC	KRCC
(1)	✓		✓		0.864	0.866	0.726	0.870	0.868	0.727	0.556	0.572	0.432	0.616	0.620	0.492
(2)	✓			✓	0.874	0.876	0.723	0.875	0.876	0.736	0.558	0.573	0.431	0.723	0.734	0.533
(3)	✓		✓	✓	0.887	0.884	0.722	0.881	0.883	0.706	0.562	0.575	0.433	0.739	0.758	0.544
(4)	✓	✓	✓		0.887	0.888	0.753	0.917	0.910	0.796	0.569	0.536	0.438	0.688	0.673	0.557
(5)	✓	✓		✓	0.905	0.908	0.754	0.919	0.917	0.799	0.589	0.587	0.441	0.742	0.763	0.549
(6)	✓	✓	✓	✓	<b>0.916</b>	<b>0.919</b>	<b>0.758</b>	<b>0.923</b>	<b>0.922</b>	<b>0.804</b>	<b>0.609</b>	<b>0.608</b>	<b>0.444</b>	<b>0.750</b>	<b>0.770</b>	<b>0.559</b>

ation perspectives. Vision-language pre-training methods such as CLIPScore [20] and BLIPScore [36] demonstrate moderate performance but are still surpassed by more specialized and fine-tuned VQA models. Specifically, deep learning-based models like FAST-VQA [69] and DOVER [70] achieve more competitive performances after fine-tuning. However, they are still far away from satisfactory. Notably, most VQA models perform better on quality evaluation than on text-video correspondence, as they lack text prompts input used in video generation, making it challenging to extract relation features from the AI-generated videos, which inevitably leads to the performance drop. Finally, the performance exploration of recent LMMs on our database shows that current LMMs are able to produce meaningful evaluations, which can motivate future works to further explore the use of LMMs for AIGV assessment.

The proposed AIGV-Assessor achieves the best performance compared to the competitors for both MOS prediction and pair ranking tasks in terms of all four dimensions. To further validate the effectiveness and generalizability of our proposed model, we also evaluate it on four other AIGVQA datasets [11, 30, 42, 84]. From Tables 4-6, we observe that AIGV-Assessor consistently achieves the best performance across these datasets. As shown in Figure 6, AIGV-Assessor achieves the highest overlap in area with Ground Truth (GT), indicating that AIGV-Assessor can reliably perform T2V model benchmarking, outperforming other assessment models in discerning quality differences in AI-generated videos.

### 5.3. Ablation Study

We conduct ablation experiments to verify the effectiveness of the main components in our AIGV-Assessor method, including the spatial feature, the temporal feature, the quality level, and the LoRA finetuning strategy. Additionally,

we assess how each feature contributes to the performance across different quality dimensions. The results of these experiments are summarized in Table 7. Experiments (1), (2), and (3) validate the effectiveness of the quality regression module and the LoRA finetuning strategy, confirming that fine-tuning and quality regression significantly enhance model performance over only regressing the generated text outputs from the LLM. The addition of temporal features, as seen in Experiments (4), (5), and (6), significantly improves model performance. Experiment (6), which integrates all components, yields the best overall performance, showing that the combination of spatial and temporal features, quality level prediction, and LoRA finetuning provides the most robust and accurate AIGV assessment.

## 6. Conclusion

In this paper, we study the human visual preference evaluation problem for AIGVs. We first construct AIGVQA-DB, which includes 36,576 videos generated based on 1048 various text-prompts, with the MOSs and pair comparisons evaluated from four perspectives. Our detailed manual evaluations reflect different aspects of human visual preferences on AIGVs and reveal critical insights into the strengths and weaknesses of various text-to-video models. Based on the database, we evaluate the performance of state-of-the-art quality evaluation models and establish a new benchmark, revealing their limitations in measuring the perceptual preference of AIGVs. Finally, we propose AIGV-Assessor, a novel VQA model that leverages the capabilities of LMMs to give quality levels, predict quality scores, and compare preferences from four dimensions. Extensive experiments demonstrate that AIGV-Assessor achieves state-of-the-art performance on both AIGVQA-DB and other AIGVQA benchmarks, validating its robustness in understanding and evaluating the AI-generated videos.



## References

- [1] Hotshot-XL. <https://github.com/hotshotco/hotshot-xl>, 2023. 2, 3, 15, 18
- [2] Floor33. <https://discord.gg/EuB9KT6H>, 2023. 2, 3, 15, 18
- [3] Gemo. <https://www.genmo.ai>, 2024. 2, 3, 15, 18
- [4] Gen2. <https://research.runwayml.com/gen2>, 2024. 2, 3, 15, 18
- [5] Moonvalley. <https://moonvalley.ai>, 2024. 2, 3, 15, 18
- [6] Morph studio. <https://www.morphstudio.com>, 2024. 2, 3, 5, 15, 18
- [7] Sora. <https://openai.com/research/video-generation-models-as-world-simulators>, 2024. 2, 3, 5, 13, 15, 18
- [8] Max Bain, Arsha Nagrani, Gül Varol, and Andrew Zisserman. Frozen in time: A joint video and image encoder for end-to-end retrieval. In *Proceedings of the IEEE/CVF International Conference on Computer Vision (ICCV)*, pages 1728–1738, 2021. 2, 3, 13, 22
- [9] Andreas Blattmann, Tim Dockhorn, Sumith Kulal, Daniel Mendelevitch, Maciej Kilian, Dominik Lorenz, Yam Levi, Zion English, Vikram Voleti, Adam Letts, et al. Stable video diffusion: Scaling latent video diffusion models to large datasets. *arXiv preprint arXiv:2311.15127*, 2023. 2, 5, 15, 18
- [10] Haoxin Chen, Menghan Xia, Yingqing He, Yong Zhang, Xiaodong Cun, Shaoshu Yang, Jinbo Xing, Yaofang Liu, Qifeng Chen, Xintao Wang, Chao Weng, and Ying Shan. Videocrafter1: Open diffusion models for high-quality video generation. *arXiv preprint arXiv:2310.19512*, 2023. 1, 2, 15, 18
- [11] Zijian Chen, Wei Sun, Yuan Tian, Jun Jia, Zicheng Zhang, Jiarui Wang, Ru Huang, Xiongkuo Min, Guangtao Zhai, and Wenjun Zhang. Gaia: Rethinking action quality assessment for ai-generated videos. *arXiv preprint arXiv:2406.06087*, 2024. 3, 7, 8
- [12] Zesen Cheng, Sicong Leng, Hang Zhang, Yifei Xin, Xin Li, Guanzheng Chen, Yongxin Zhu, Wenqi Zhang, Ziyang Luo, Deli Zhao, and Lidong Bing. Videollama 2: Advancing spatial-temporal modeling and audio understanding in video-llms. *arXiv preprint arXiv:2406.07476*, 2024. 6, 7
- [13] Shyamprasad Chikkerur, Vijay Sundaram, Martin Reisslein, and Lina J Karam. Objective video quality assessment methods: A classification, review, and performance comparison. *IEEE transactions on broadcasting (TBC)*, 57(2):165–182, 2011. 20
- [14] Iya Chivileva, Philip Lynch, Tomas E Ward, and Alan F Smeaton. Measuring the quality of text-to-video model outputs: Metrics and dataset. *arXiv preprint arXiv:2309.08009*, 2023. 3
- [15] Ming Ding, Wendi Zheng, Wenyi Hong, and Jie Tang. Cogview2: Faster and better text-to-image generation via hierarchical transformers. In *Proceedings of the Advances in Neural Information Processing Systems (NeurIPS)*, pages 16890–16902, 2022. 3, 14
- [16] Huiyu Duan, Xiongkuo Min, Yucheng Zhu, Guangtao Zhai, Xiaokang Yang, and Patrick Le Callet. Confusing image quality assessment: Toward better augmented reality experience. *IEEE Transactions on Image Processing (TIP)*, 31: 7206–7221, 2022. 4
- [17] Christoph Feichtenhofer, Haoqi Fan, Jitendra Malik, and Kaiming He. Slowfast networks for video recognition. In *Proceedings of the IEEE/CVF International Conference on Computer Vision (ICCV)*, pages 6202–6211, 2019. 5
- [18] Yuwei Guo, Ceyuan Yang, Anyi Rao, Yaohui Wang, Yu Qiao, Dahua Lin, and Bo Dai. Animatediff: Animate your personalized text-to-image diffusion models without specific tuning. *arXiv preprint arXiv:2307.04725*, 2023. 2
- [19] Yingqing He, Tianyu Yang, Yong Zhang, Ying Shan, and Qifeng Chen. Latent video diffusion models for high-fidelity video generation with arbitrary lengths. *arXiv preprint arXiv:2211.13221*, 2022. 2, 3, 5, 14, 15, 18
- [20] Jack Hessel, Ari Holtzman, Maxwell Forbes, Ronan Le Bras, and Yejin Choi. Clipscore: A reference-free evaluation metric for image captioning. In *Proceedings of the Conference on Empirical Methods in Natural Language Processing (EMNLP)*, pages 7514–7528, 2021. 1, 6, 7, 8, 20
- [21] Jonathan Ho, Ajay Jain, and Pieter Abbeel. Denoising diffusion probabilistic models. 33:6840–6851, 2020. 15
- [22] Wenyi Hong, Ming Ding, Wendi Zheng, Xinghan Liu, and Jie Tang. Cogvideo: Large-scale pretraining for text-to-video generation via transformers. *arXiv preprint arXiv:2205.15868*, 2022. 1, 2, 3, 14, 15
- [23] Edward J Hu, Yelong Shen, Phillip Wallis, Zeyuan Allen-Zhu, Yuanzhi Li, Shean Wang, Lu Wang, and Weizhu Chen. Lora: Low-rank adaptation of large language models. *arXiv preprint arXiv:2106.09685*, 2021. 6
- [24] Ziqi Huang, Yinan He, Jiashuo Yu, Fan Zhang, Chenyang Si, Yuming Jiang, Yuanhan Zhang, Tianxing Wu, Qingyang Jin, Nattapol Chanpaisit, Yaohui Wang, Xinyuan Chen, Limin Wang, Dahua Lin, Yu Qiao, and Ziwei Liu. VBench: Comprehensive benchmark suite for video generative models. In *Proceedings of the IEEE/CVF Conference on Computer Vision and Pattern Recognition (CVPR)*, 2024. 1, 6, 7, 20
- [25] Junjie Ke, Qifei Wang, Yilin Wang, Peyman Milanfar, and Feng Yang. Musiq: Multi-scale image quality transformer. In *Proceedings of the IEEE/CVF International Conference on Computer Vision (ICCV)*, pages 5128–5137, 2021. 6, 7
- [26] Levon Khachatryan, Andranik Movsisyan, Vahram Tadevosyan, Roberto Henschel, Zhangyang Wang, Shant Navasardyan, and Humphrey Shi. Text2video-zero: Text-to-image diffusion models are zero-shot video generators. In *Proceedings of the IEEE/CVF International Conference on Computer Vision (ICCV)*, pages 15954–15964, 2023. 1, 2, 3, 15, 18
- [27] Yuval Kirstain, Adam Poliak, Uriel Singer, and Omer Levy. Pick-a-pic: An open dataset of user preferences for text-to-image generation. In *Proceedings of the Advances in Neural Information Processing Systems (NeurIPS)*, 2023. 7
- [28] Yuval Kirstain, Adam Polyak, Uriel Singer, Shahbuland Matiana, Joe Penna, and Omer Levy. Pick-a-pic: An open dataset of user preferences for text-to-image generation. In

- Proceedings of the Advances in Neural Information Processing Systems (NeurIPS)*, pages 36652–36663, 2023. 3, 13
- [29] Jari Korhonen. Two-level approach for no-reference consumer video quality assessment. *IEEE Transactions on Image Processing (TIP)*, 28(12):5923–5938, 2019. 7
- [30] Tengchuan Kou, Xiaohong Liu, Zicheng Zhang, Chunyi Li, Haoning Wu, Xiongkuo Min, Guangtao Zhai, and Ning Liu. Subjective-aligned dataset and metric for text-to-video quality assessment. *arXiv preprint arXiv:2403.11956*, 2024. 1, 3, 7, 8
- [31] Debarati Kundu, Deepti Ghadiyaram, Alan C Bovik, and Brian L Evans. Large-scale crowdsourced study for tone-mapped hdr pictures. *IEEE Transactions on Image Processing (TIP)*, pages 4725–4740, 2017. 7
- [32] Bowen Li, Weixia Zhang, Meng Tian, Guangtao Zhai, and Xianpei Wang. Blindly assess quality of in-the-wild videos via quality-aware pre-training and motion perception. *IEEE Transactions on Circuits and Systems for Video Technology (TCSVT)*, 32(9):5944–5958, 2022. 1, 6, 7, 20
- [33] Chunyi Li, Zicheng Zhang, Haoning Wu, Wei Sun, Xiongkuo Min, Xiaohong Liu, Guangtao Zhai, and Weisi Lin. Agiqa-3k: An open database for ai-generated image quality assessment. *IEEE Transactions on Circuits and Systems for Video Technology (TCSVT)*, 2023. 3
- [34] Dingquan Li, Tingting Jiang, and Ming Jiang. Quality assessment of in-the-wild videos. In *Proceedings of the ACM International Conference on Multimedia (ACMMM)*. ACM, 2019. 1, 6, 7, 20
- [35] Feng Li, Renrui Zhang, Hao Zhang, Yuanhan Zhang, Bo Li, Wei Li, Zejun Ma, and Chunyuan Li. Llava-next-interleave: Tackling multi-image, video, and 3d in large multimodal models. *arXiv preprint arXiv:2407.07895*, 2024. 6, 7
- [36] Junnan Li, Dongxu Li, Caiming Xiong, and Steven Hoi. Blip: Bootstrapping language-image pre-training for unified vision-language understanding and generation. In *Proceedings of the International Conference on Machine Learning (ICML)*, pages 12888–12900. PMLR, 2022. 1, 6, 7, 8, 20
- [37] Yuncheng Li, Yale Song, Liangliang Cao, Joel Tetreault, Larry Goldberg, Alejandro Jaimes, and Jiebo Luo. Tgif: A new dataset and benchmark on animated gif description. In *Proceedings of the IEEE/CVF Conference on Computer Vision and Pattern Recognition (CVPR)*, pages 4641–4650, 2016. 2, 3, 13, 22
- [38] Youwei Liang, Junfeng He, Gang Li, Peizhao Li, Arseniy Klimovskiy, Nicholas Carolan, Jiao Sun, Jordi Pont-Tuset, Sarah Young, Feng Yang, et al. Rich human feedback for text-to-image generation. In *Proceedings of the IEEE/CVF Conference on Computer Vision and Pattern Recognition (CVPR)*, pages 19401–19411, 2024. 1, 3
- [39] Bin Lin, Bin Zhu, Yang Ye, Munan Ning, Peng Jin, and Li Yuan. Video-llava: Learning united visual representation by alignment before projection. *arXiv preprint arXiv:2311.10122*, 2023. 6, 7
- [40] Haotian Liu, Chunyuan Li, Qingyang Wu, and Yong Jae Lee. Visual instruction tuning. In *Proceedings of the Advances in Neural Information Processing Systems (NeurIPS)*, 2024. 7
- [41] Yaofang Liu, Xiaodong Cun, Xuebo Liu, Xintao Wang, Yong Zhang, Haoxin Chen, Yang Liu, Tiejiong Zeng, Raymond Chan, and Ying Shan. Evalcrafter: Benchmarking and evaluating large video generation models. *arXiv preprint arXiv:2310.11440*, 2023. 3, 7
- [42] Yuanxin Liu, Lei Li, Shuhuai Ren, Rundong Gao, Shicheng Li, Sishuo Chen, Xu Sun, and Lu Hou. Fetv: A benchmark for fine-grained evaluation of open-domain text-to-video generation. In *Proceedings of the Advances in Neural Information Processing Systems (NeurIPS)*, 2024. 1, 2, 3, 6, 7, 8, 13, 22
- [43] Zhengxiong Luo, Dayou Chen, Yingya Zhang, Yan Huang, Liang Wang, Yujun Shen, Deli Zhao, Jingren Zhou, and Tieniu Tan. Videofusion: Decomposed diffusion models for high-quality video generation. In *Proceedings of the IEEE/CVF Conference on Computer Vision and Pattern Recognition (CVPR)*, pages 10209–10218, 2023. 1, 2, 3, 15, 18
- [44] Muhammad Maaz, Hanoona Rasheed, Salman Khan, and Fahad Shahbaz Khan. Video-chatgpt: Towards detailed video understanding via large vision and language models. In *Proceedings of the Association for Computational Linguistics (ACL)*, 2024. 6, 7
- [45] Xiongkuo Min, Ke Gu, Guangtao Zhai, Jing Liu, Xiaokang Yang, and Chang Wen Chen. Blind quality assessment based on pseudo-reference image. *IEEE Transactions on Multimedia (TMM)*, pages 2049–2062, 2017. 6, 7
- [46] Xiongkuo Min, Guangtao Zhai, Ke Gu, Yutao Liu, and Xiaokang Yang. Blind image quality estimation via distortion aggravation. *IEEE Transactions on Broadcasting (TBC)*, pages 508–517, 2018. 6, 7
- [47] Anish Mittal, Anush Krishna Moorthy, and Alan Conrad Bovik. No-reference image quality assessment in the spatial domain. *IEEE Transactions on Image Processing (TIP)*, pages 4695–4708, 2012. 6, 7
- [48] Anish Mittal, Rajiv Soundararajan, and Alan C Bovik. Making a “completely blind” image quality analyzer. *IEEE Signal Processing Letters (SPL)*, pages 209–212, 2012. 6, 7
- [49] Paritosh Parmar and Brendan Tran Morris. What and how well you performed? a multitask learning approach to action quality assessment. In *Proceedings of the IEEE/CVF Conference on Computer Vision and Pattern Recognition (CVPR)*, pages 304–313, 2019. 20
- [50] Ekta Prashnani, Hong Cai, Yasamin Mostofi, and Pradeep Sen. Pieapp: Perceptual image-error assessment through pairwise preference. In *Proceedings of the IEEE/CVF Conference on Computer Vision and Pattern Recognition (CVPR)*, pages 1808–1817, 2018. 13
- [51] Aditya Ramesh, Prafulla Dhariwal, Alex Nichol, Casey Chu, and Mark Chen. Hierarchical text-conditional image generation with clip latents. *arXiv preprint arXiv:2204.06125*, 1(2):3, 2022. 3
- [52] Robin Rombach, Andreas Blattmann, Dominik Lorenz, Patrick Esser, and Björn Ommer. High-resolution image synthesis with latent diffusion models. In *Proceedings of the IEEE/CVF Conference on Computer Vision and Pattern Recognition (CVPR)*, pages 10684–10695, 2022. 3

- [53] Tim Salimans, Ian Goodfellow, Wojciech Zaremba, Vicki Cheung, Alec Radford, and Xi Chen. Improved techniques for training gans. In *Proceedings of the Advances in Neural Information Processing Systems (NeurIPS)*, 2016. 1
- [54] Christoph Schuhmann, Romain Beaumont, Richard Vencu, Cade Gordon, Ross Wightman, Mehdi Cherti, Theo Coombes, Aarush Katta, Clayton Mullis, Mitchell Wortsman, et al. Laion-5b: An open large-scale dataset for training next generation image-text models. In *Proceedings of the Advances in Neural Information Processing Systems (NeurIPS)*, pages 25278–25294, 2022. 1, 6, 7, 20
- [55] Uriel Singer, Adam Polyak, Thomas Hayes, Xi Yin, Jie An, Songyang Zhang, Qiyuan Hu, Harry Yang, Oron Ashual, Oran Gafni, et al. Make-a-video: Text-to-video generation without text-video data. *arXiv preprint arXiv:2209.14792*, 2022. 1, 2, 3
- [56] Shaolin Su, Qingsen Yan, Yu Zhu, Cheng Zhang, Xin Ge, Jinqiu Sun, and Yanning Zhang. Blindly assess image quality in the wild guided by a self-adaptive hyper network. In *IEEE/CVF Conference on Computer Vision and Pattern Recognition (CVPR)*, 2020. 6, 7
- [57] Wei Sun, Xiongkuo Min, Wei Lu, and Guangtao Zhai. A deep learning based no-reference quality assessment model for ugc videos. In *Proceedings of the 30th ACM International Conference on Multimedia (ACMMM)*, page 856–865, 2022. 1, 6, 7, 21
- [58] Wei Sun, Xiongkuo Min, Wei Lu, and Guangtao Zhai. A deep learning based no-reference quality assessment model for ugc videos. In *Proceedings of the ACM International Conference on Multimedia (ACMMM)*, pages 856–865, 2022. 7
- [59] Wei Sun, Xiongkuo Min, Danyang Tu, Siwei Ma, and Guangtao Zhai. Blind quality assessment for in-the-wild images via hierarchical feature fusion and iterative mixed database training. *IEEE Journal of Selected Topics in Signal Processing (JSTSP)*, 2023. 7
- [60] Zhengzhong Tu, Yilin Wang, Neil Birkbeck, Balu Adsumilli, and Alan C Bovik. Ugc-vqa: Benchmarking blind video quality assessment for user generated content. *IEEE Transactions on Image Processing (TIP)*, 30:4449–4464, 2021. 7
- [61] Thomas Unterthiner, Sjoerd Van Steenkiste, Karol Kurach, Raphael Marinier, Marcin Michalski, and Sylvain Gelly. Towards accurate generative models of video: A new metric & challenges. *arXiv preprint arXiv:1812.01717*, 2018. 1
- [62] Jianyi Wang, Kelvin C.K. Chan, and Chen Change Loy. Exploring clip for assessing the look and feel of images. In *Proceedings of the AAAI Conference on Artificial Intelligence (AAAI)*, pages 2555–2563, 2023. 7
- [63] Jiarui Wang, Huiyu Duan, Jing Liu, Shi Chen, Xiongkuo Min, and Guangtao Zhai. Aigciqa2023: A large-scale image quality assessment database for ai generated images: from the perspectives of quality, authenticity and correspondence. In *CAAI International Conference on Artificial Intelligence (CICAI)*, pages 46–57. Springer, 2023. 3
- [64] Jiumiu Wang, Hangjie Yuan, Dayou Chen, Yingya Zhang, Xiang Wang, and Shiwei Zhang. Modelscope text-to-video technical report. *arXiv preprint arXiv:2308.06571*, 2023. 1, 2, 3
- [65] Peng Wang, Shuai Bai, Sinan Tan, Shijie Wang, Zhihao Fan, Jinze Bai, Keqin Chen, Xuejing Liu, Jialin Wang, Wenbin Ge, Yang Fan, Kai Dang, Mengfei Du, Xuancheng Ren, Rui Men, Dayiheng Liu, Chang Zhou, Jingren Zhou, and Junyang Lin. Qwen2-vl: Enhancing vision-language model’s perception of the world at any resolution. *arXiv preprint arXiv:2409.12191*, 2024. 6, 7
- [66] Yaohui Wang, Xinyuan Chen, Xin Ma, Shangchen Zhou, Ziqi Huang, Yi Wang, Ceyuan Yang, Yinan He, Jiashuo Yu, Peiqing Yang, et al. Lavie: High-quality video generation with cascaded latent diffusion models. *arXiv preprint arXiv:2309.15103*, 2023. 2, 3, 15
- [67] Yi Wang, Yinan He, Yizhuo Li, Kunchang Li, Jiashuo Yu, Xin Ma, Xinhao Li, Guo Chen, Xinyuan Chen, Yaohui Wang, et al. Internvid: A large-scale video-text dataset for multimodal understanding and generation. In *Proceedings of the International Conference on Learning Representations (ICLR)*, 2023. 2, 3, 13, 22
- [68] Zirui Wang, Mengzhou Xia, Luxi He, Howard Chen, Yitao Liu, Richard Zhu, Kaiqu Liang, Xindi Wu, Haotian Liu, Sadhika Malladi, Alexis Chevalier, Sanjeev Arora, and Danqi Chen. Charxiv: Charting gaps in realistic chart understanding in multimodal llms. *arXiv preprint arXiv:2406.18521*, 2024. 5, 6
- [69] Haoning Wu, Chaofeng Chen, Jingwen Hou, Liang Liao, Annan Wang, Wenxiu Sun, Qiong Yan, and Weisi Lin. Fastvqa: Efficient end-to-end video quality assessment with fragment sampling. In *Proceedings of the European Conference on Computer Vision (ECCV)*, pages 538–554. Springer, 2022. 1, 6, 7, 8, 21
- [70] Haoning Wu, Erli Zhang, Liang Liao, Chaofeng Chen, Jingwen Hou, Annan Wang, Wenxiu Sun, Qiong Yan, and Weisi Lin. Exploring video quality assessment on user generated contents from aesthetic and technical perspectives. In *Proceedings of the International Conference on Computer Vision (ICCV)*, 2023. 1, 6, 7, 8, 21
- [71] Haoning Wu, Zicheng Zhang, Weixia Zhang, Chaofeng Chen, Liang Liao, Chunyi Li, Yixuan Gao, Annan Wang, Erli Zhang, Wenxiu Sun, et al. Q-align: Teaching llms for visual scoring via discrete text-defined levels. *arXiv preprint arXiv:2312.17090*, 2023. 6, 7, 21
- [72] Jay Zhangjie Wu, Yixiao Ge, Xintao Wang, Stan Weixian Lei, Yuchao Gu, Yufei Shi, Wynne Hsu, Ying Shan, Xiaohu Qie, and Mike Zheng Shou. Tune-a-video: One-shot tuning of image diffusion models for text-to-video generation. In *Proceedings of the IEEE/CVF International Conference on Computer Vision (ICCV)*, pages 7623–7633, 2023. 1, 2, 3, 15, 18
- [73] Xiaoshi Wu, Yiming Hao, Keqiang Sun, Yixiong Chen, Feng Zhu, Rui Zhao, and Hongsheng Li. Human preference score v2: A solid benchmark for evaluating human preferences of text-to-image synthesis. *arXiv preprint arXiv:2306.09341*, 2023. 7
- [74] Xiaoshi Wu, Keqiang Sun, Feng Zhu, Rui Zhao, and Hongsheng Li. Better aligning text-to-image models with human preference. *arXiv preprint arXiv:2303.14420*, 1(3), 2023. 3, 13

- [75] Jun Xu, Tao Mei, Ting Yao, and Yong Rui. Msr-vtt: A large video description dataset for bridging video and language. In *Proceedings of the IEEE/CVF Conference on Computer Vision and Pattern Recognition (CVPR)*, 2016. [2](#), [3](#), [13](#), [22](#)
- [76] Jingtao Xu, Peng Ye, Qiaohong Li, Haiqing Du, Yong Liu, and David Doermann. Blind image quality assessment based on high order statistics aggregation. *IEEE Transactions on Image Processing (TIP)*, pages 4444–4457, 2016. [6](#), [7](#)
- [77] Jiazheng Xu, Xiao Liu, Yuchen Wu, Yuxuan Tong, Qinkai Li, Ming Ding, Jie Tang, and Yuxiao Dong. Imagereward: Learning and evaluating human preferences for text-to-image generation. *arXiv preprint arXiv:2304.05977*, 2023. [6](#), [7](#)
- [78] Jiazheng Xu, Xiao Liu, Yuchen Wu, Yuxuan Tong, Qinkai Li, Ming Ding, Jie Tang, and Yuxiao Dong. Imagereward: Learning and evaluating human preferences for text-to-image generation. In *Proceedings of the Advances in Neural Information Processing Systems (NeurIPS)*, 2024. [1](#)
- [79] Wufeng Xue, Lei Zhang, and Xuanqin Mou. Learning without human scores for blind image quality assessment. In *Proceedings of the IEEE/CVF Conference on Computer Vision and Pattern Recognition (CVPR)*, pages 995–1002, 2013. [6](#), [7](#)
- [80] Wilson Yan, Yunzhi Zhang, Pieter Abbeel, and Aravind Srinivas. Videogpt: Video generation using vq-vae and transformers. *arXiv preprint arXiv:2104.10157*, 2021. [1](#)
- [81] Richard Zhang, Phillip Isola, Alexei A Efros, Eli Shechtman, and Oliver Wang. The unreasonable effectiveness of deep features as a perceptual metric. In *Proceedings of the IEEE/CVF Conference on Computer Vision and Pattern Recognition (CVPR)*, pages 586–595, 2018. [6](#), [13](#)
- [82] Wenlong Zhang, Yihao Liu, Chao Dong, and Yu Qiao. Rankrgan: Generative adversarial networks with ranker for image super-resolution. In *Proceedings of the IEEE/CVF Conference on Computer Vision and Pattern Recognition (CVPR)*, pages 3096–3105, 2019. [13](#)
- [83] Weixia Zhang, Guangtao Zhai, Ying Wei, Xiaokang Yang, and Kede Ma. Blind image quality assessment via vision-language correspondence: A multitask learning perspective. In *Proceedings of the IEEE/CVF Conference on Computer Vision and Pattern Recognition (CVPR)*, 2023. [6](#), [7](#)
- [84] Zhichao Zhang, Xinyue Li, Wei Sun, Jun Jia, Xiongkuo Min, Zicheng Zhang, Chunyi Li, Zijian Chen, Puyi Wang, Zhongpeng Ji, et al. Benchmarking aigc video quality assessment: A dataset and unified model. *arXiv preprint arXiv:2407.21408*, 2024. [1](#), [3](#), [7](#), [8](#)

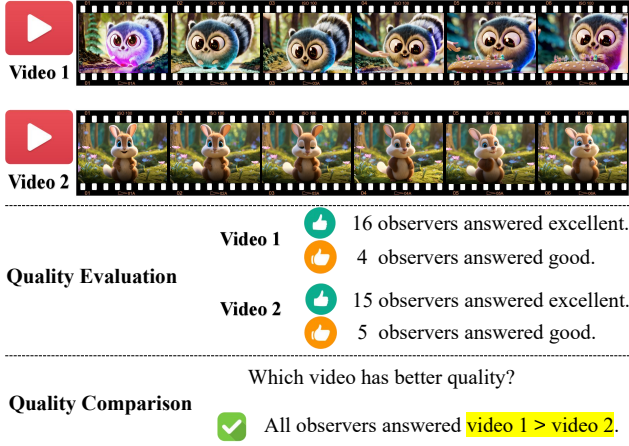


Figure 7. The motivation for visual quality comparison: single stimulus absolute ratings like “excellent” or “good” often involve randomness or inconsistency due to varying personal standards. Double stimuli comparative settings avoid the ambiguity of absolute evaluations for single videos, providing clearer and more consistent judgments.

## A. Significance of AIGVQA-DB Construction

Mean opinion scores (MOS) have traditionally served as the primary metric for measuring overall quality. While MOS is effective for providing a general indication of quality, it has notable limitations, especially when it comes to high-quality content. For example, when evaluating closely matched, high-quality images or videos, MOS often results in similar scores across samples, leading to coarse evaluations that fail to capture subtle differences in factors like exposure, motion smoothness, or color fidelity. As illustrated in Figure 7, human assessors applying absolute scoring frequently yield inconsistent ratings due to varying personal standards or subjective preferences. Despite this, when asked to make relative comparisons—such as deciding whether “video1 is better than video2”—they exhibit greater consistency and are able to reach a reliable consensus. This highlights a crucial insight: relative comparisons offer more precision and consistency than absolute scoring alone. Pairwise comparisons, which focus on directly comparing two samples, have thus emerged as a valuable complement to MOS. By emphasizing relative differences, pairwise assessments allow for finer granularity, capturing nuanced distinctions that absolute scores may miss. Numerous studies have demonstrated the effectiveness of pairwise comparisons in reducing ambiguity in scoring and providing more detailed evaluations, especially when assessing high-quality content [28, 50, 74, 81, 82].

The development of AI-generated image quality assessment (AIGIQA) datasets is already relatively well-established, incorporating both MOS for absolute quality evaluation and pairwise comparisons for assessing relative quality differences. This dual approach has proven ef-

fective in capturing both the overall and relative quality aspects of AI-generated images. However, existing AI-generated video quality assessment (AIGVQA) datasets primarily rely on MOS alone, which significantly limits their ability to capture the fine-grained quality differences inherent in video content. Videos, unlike static images, present unique challenges such as temporal coherence, spatial consistency, and the dynamic nature of objects and motion. These challenges make pairwise comparisons particularly valuable in video quality assessment, as they allow for more accurate evaluations of complex attributes like motion smoothness and frame-to-frame consistency. Unfortunately, most current VQA datasets lack systematic, large-scale pairwise data, limiting their capacity to assess these dynamic and temporal aspects effectively. To address this gap, we propose the AIGVQA-DB dataset, including both MOS and pairwise comparison data, offering a robust framework for evaluating the intricate nuances of AI-generated video content. By incorporating both absolute quality judgments and relative assessments, AIGVQA-DB enables more accurate model training and evaluation, allowing models to learn not only the absolute quality standards but also the relational nuances inherent in video sequences.

## B. More Details of Video Generation

### B.1. Detailed Information of Prompts

The AIGVQA-DB dataset offers a rich and diverse collection of prompts, carefully constructed from two sources: (1) existing open-domain text-video pair datasets, including InternVid [67], MSRVT [75], WebVid [8], TGIF [37], FETV [42] and Sora website [7]. These datasets contribute a robust foundation of real-world and generalizable scenarios, providing a solid basis for training and evaluation. (2) manually written prompts designed to push the boundaries of model robustness and generalization. Inspired by unique categories such as “Imagination” and “Conflicting,” these prompts introduce rare or non-realistic scenarios, like “A panda is flying in the sky,” that test a model’s ability to handle creative and unconventional inputs. As illustrated in Table 8, each prompt in our dataset is categorized based on four key aspects, including “spatial major content”, “temporal major content”, “attribute control”, and “prompt complexity”. For each aspect, we include typical elements that frequently occur in daily life. As shown in Figure 5, the spatial major content focuses on objects described in the prompt, including ten subcategories: people, animals, plants, and *etc.* In contrast, temporal major content highlights dynamic actions or changes and is divided into four subcategories, including actions, kinetic motions, fluid motions, and light change, as shown in Figure 6. Similarly, the attribute control covers specific stylistic or compositional controls embedded in prompts, en-

Table 8. Prompt categorizations with subcategories, detailed descriptions, and representative keyword examples.

Category	Subcategory	Descriptions	Keyword examples
Spatial major content	People	Prompts that include humans.	person, man, woman, men, women, kid, girl, boy, baby
	Plants	Prompts that include plants.	flower, leaf, tree, grass, forest, wheat, plant, peony
	Animals	Prompts that include animals.	panda, dog, cat, elephant, horse, bird, butterfly, rabbit
	Vehicles	Prompts that include vehicles.	car, van, plane, tank, carriage, rocket, motorcycle
	Artifacts	Prompts that include human-made objects.	robot, doll, toy, microphone, paper, plate, bowl, ball
	Illustrations	Prompts that include geometrical objects and symbols.	abstract, pattern, particle, gradient, loop, graphic, line
	Food and beverage	Prompts that include food and beverage.	water, wine, coffee, apple, butter, egg, chocolate, lime
Temporal major content	Buildings and infrastructure	Prompts that include buildings and infrastructure.	room, building, bridge, court, concert, hotel, factory
	Scenery and natural objects	Prompts that include lifeless natural objects and scenery.	wind, sand, snow, rain, sky, fog, mountain, river, sun
	Actions	Prompts that include the motion of solid objects	sing, dance, laugh, cry, smile, jump, walk, eat, drink
	Kinetic motions	Prompts that include the motion of solid objects.	fly, spin, race, move, rotate, fall, rise, bounce, sway
Attribute control	Fluid motions	Prompts that include the motions of fluids or like fluids.	waterfall, wave, fountain, smoke, steam, inflate, melt
	Light change	Prompts from which the generated videos may involve light change.	sunset, sunrise, firework, shine, glow, burn, flash, bright
	Color	Prompts that include colors.	white, pink, black, red, green, purple, blue, yellow
	Quantity	Prompts that include numbers.	one, two, three, four, five, six, seven, eight, nine, ten
	Camera view	Prompts that include control over the camera view.	view, macro, film, close, capture, aerial, shot, camera
	Speed	Prompts that include control over speed.	fast, slow, rapid, speed, motion, time, quick, swift, lag
Prompt complexity	Event order	Prompts that include control over the order of events.	then, before, after, first, second
	Motion direction	Prompts that include control over the motion direction.	forward, backward, from, into, through, out of, left, right
	Simple	Prompts that involve 0 ~ 8 non-stop words.	-
Medium	Prompts that involve 9 ~ 11 non-stop words.	-	
Complex	Prompts that involve more than 11 non-stop words.	-	

abling nuanced customization of generated content, including color, quantity, camera view, speed, motion direction, and event order, as shown in Figure 7. Additionally, we classify prompt complexity into three levels including: simple, medium, and complex, based on the number of descriptive elements in the text. By integrating real-world scenarios, imaginative constructs, and a structured categorization system, AIGVQA-DB ensures a comprehensive evaluation framework that challenges text-to-video generation models in both realistic and highly creative contexts.

To ensure a comprehensive and systematic classification of prompts within the AIGVQA-DB dataset, we employed the GPT-4 API for multi-aspect prompt categorization. GPT-4 was provided with task-specific instructions designed to guide its classification process. These instructions included detailed descriptions of the categorization task, along with illustrative examples to ensure consistent and accurate labeling. Prompts were analyzed based on key aspects. For instance, to classify spatial major content, GPT-4 was prompted with a detailed instruction template, such as:

*"Analyze the following prompt and classify it into one or more categories based on the type of object it describes. The categories include People, Buildings and Infrastructure, Animals, Artifacts, Vehicles, Plants, Scenery and Natural Objects, Food and Beverage, and Illustration. Provide only the category names as the output. Example: 'A cat is sitting under a tree.' Spatial major content: Animals, Plants."*

Under this framework, GPT-4 processes the given

prompt and assigns appropriate category labels based on its analysis. For example, a prompt like "A dog is driving a car." would be classified under Animals and Vehicles. Similar categorization instructions were devised for temporal major content and attribute control. Additionally, prompt complexity is classified based on the number of non-stop words present in each prompt. This multi-aspect categorization approach ensured that every prompt in the AIGVQA-DB was exhaustively labeled, facilitating fine-grained evaluation of text-to-video models. Examples of prompts and their corresponding categorizations in AIGVQA-DB are shown in Table 10.

## B.2. Detailed Information of Text-to-Video Models

To construct AIGVQA-DB, we utilize 15 state-of-the-art text-to-video generative models, encompassing both open-source and closed-source methods, as detailed in Table 9. For open-source models, we rely on official repositories and use default weights to standardize results and maintain consistency across experiments. For closed-source models, we leverage publicly available APIs from open-source platforms. This comprehensive selection ensures that AIGVQA-DB serves as a robust benchmark for evaluating text-to-video generation systems.

**CogVideo.** CogVideo [22] is built on the text-to-image model CogView2 [15]. It employs a multi-frame-rate hierarchical training strategy to ensure better alignment between text and temporal counterparts in videos, generating keyframes based on textual prompts and recursively interpolating intermediate frames for coherence.

**LVDM.** LVDM [19] is an efficient video diffusion model operating in a compressed latent space, designed to address the computational challenges of video synthesis. It uses a

Table 9. Video formats and numbers generated by the 15 text-to-video (T2V) models in the AIGVQA-DB. ✓ in the Pairs and MOS columns indicate which generative models are utilized in each of the two subsets. † Representative variable. \*Representative open-source.

Models	Number	Prompts	Frames	FPS	Resolution	MOS	Pairs	URL
*CogVideo [22]	4,000	1,000	32	10	480×480	-	✓	<a href="https://github.com/THUDM/CogVideo">https://github.com/THUDM/CogVideo</a>
*LVDM [19]	4,048	1,048	16	8	256×256	✓	✓	<a href="https://github.com/YingqingHe/LVDM">https://github.com/YingqingHe/LVDM</a>
*Tune-A-Video [72]	4,048	1,048	8	8	512×512	✓	✓	<a href="https://github.com/showlab/Tune-A-Video">https://github.com/showlab/Tune-A-Video</a>
*VideoFusion [43]	4,048	1,048	16	8	256×256	✓	✓	<a href="https://github.com/modelscope/modelscope">https://github.com/modelscope/modelscope</a>
*Text2Video-Zero [26]	4,048	1,048	8	4	512×512	✓	✓	<a href="https://github.com/Picsart-AI-Research/Text2Video-Zero">https://github.com/Picsart-AI-Research/Text2Video-Zero</a>
*LaVie [66]	4,048	1,048	16	8	512×320	✓	✓	<a href="https://github.com/Vchitect/LaVie">https://github.com/Vchitect/LaVie</a>
*VideoCrafter [10]	4,048	1,048	16	10	1024×576	✓	✓	<a href="https://github.com/AILab-CVC/VideoCrafter">https://github.com/AILab-CVC/VideoCrafter</a>
*Hotshot-XL [1]	4,048	1,048	8	8	672×384	✓	✓	<a href="https://github.com/hotshotco/Hotshot-XL">https://github.com/hotshotco/Hotshot-XL</a>
*StableVideoDiffusion [9]	1,000	1,000	14	6	576×1024	-	✓	<a href="https://github.com/Stability-AI/generative-models">https://github.com/Stability-AI/generative-models</a>
Floor33 [2]	4,048	1,048	16	8	1024×640	✓	✓	<a href="https://discord.com/invite/EuB9KT6H">https://discord.com/invite/EuB9KT6H</a>
Genmo [3]	4,048	1,048	60	15	2048×1536†	✓	✓	<a href="https://www.genmo.ai">https://www.genmo.ai</a>
Gen-2 [4]	48	48	96	24	1408×768	✓	-	<a href="https://research.runwayml.com/gen2">https://research.runwayml.com/gen2</a>
MoonValley [5]	48	48	200†	50	1184×672	✓	-	<a href="https://moonvalley.ai">https://moonvalley.ai</a>
MorphStudio [6]	4,000	1,000	72	24	1920×1080	-	✓	<a href="https://www.morphstudio.com">https://www.morphstudio.com</a>
Sora [7]	48	48	600†	30	1920×1080†	✓	-	<a href="https://openai.com/research">https://openai.com/research</a>

hierarchical framework to extend video generation beyond training lengths, effectively mitigating performance degradation via conditional latent perturbation and unconditional guidance techniques.

**Tune-A-Video.** Tune-A-Video [72] is a one-shot text-to-video generation model that extends text-to-image (T2I) models to the spatio-temporal domain. It uses sparse spatio-temporal attention to maintain consistent objects across frames, overcoming computational limitations. It can synthesize novel videos from a single example compatible with personalized and conditional pretrained T2I models.

**VideoFusion.** VideoFusion [43] is a decomposed diffusion probabilistic model for video generation. Unlike traditional methods that add independent noise to each frame, it separates noise into shared base noise and residual noise, improving spatial-temporal coherence. This approach leverages pretrained image-generation models for efficient frame content prediction while maintaining motion dynamics.

**Text2Video-Zero.** Text2Video-Zero [26] is a zero-shot text-to-video synthesis model without any further fine-tuning or optimization, which introduces motion dynamics between the latent codes and cross-frame attention mechanism to keep the global scene time consistent. We adopt its official code with default parameters (`<motion_field_strength_x&y=12>`).

**LaVie.** LaVie [66] is an integrated video generation framework that operates on cascaded video latent diffusion models. For each prompt, we use the base T2V model and sample 16 frames of size 512×320 at 8 FPS. The number of DDPM [21] sampling steps and guidance scale are set as 50 and 7.5, respectively.

**VideoCrafter.** VideoCrafter [10] is a video generation and editing toolbox. We sample 16 frames of size 1024×576 at 8 FPS, according to its default settings.

**Hotshot-XL.** Hotshot-XL [1] is a text-to-gif model trained to work alongside Stable Diffusion XL<sup>1</sup>. We adopt its of-

ficial code with default parameters and change the output format from GIF to MP4.

**Genmo.** Genmo [3] is a high-quality video generation platform. We generate 60 frames of size  $\leq 2048 \times 1536$  at 15 FPS for each prompt. The motion parameter is set to 70%.

**Gen-2.** Gen-2 [4] is a multimodal AI system, introduced by Runway AI, Inc., which can generate novel videos with text, images or video clips. We collect 96 frames of size 1408×768 at 24 FPS for each prompt.

**Sora.** Sora [7] is particularly known for its ability to handle complex, multi-element prompts, ensuring coherent visual representations of diverse scenarios. Sora [7] currently does not have an open-source API, so the videos we used are downloaded from its official website.

**Floor33, MoonValley and MorphStudio.** Floor33 [2], MoonValley [5], and MorphStudio [6] are recent popular online video generation application. We use the T2V mode of these applications via commands in Discord<sup>2</sup>.

## C. More Details of Subjective Experiment

### C.1. Annotation Criteria

The assessment criteria for AIGVQA-DB are systematically structured across four key dimensions: static quality, temporal smoothness, dynamic degree, and text-video correspondence. These dimensions provide a comprehensive framework for video quality assessment, ensuring thorough and reliable assessments through clearly defined scales, detailed annotation criteria, and illustrative reference examples.

- **Static quality** focuses on the video’s visual clarity, naturalness, color balance, and detail richness. High-scoring videos are characterized by exceptional clarity, vivid and well-balanced colors, and meticulous attention to detail, offering an immersive and visually striking experience. Conversely, low scores reflect videos with blurriness, un-

<sup>1</sup><https://huggingface.co/hotshotco/SDXL-512>

<sup>2</sup><https://discord.com>

natural color tones, faded visuals, and lack of clarity or detail. This dimension captures the foundational visual attributes that make a video aesthetically pleasing or distracting. For detailed criteria, refer to Figure 14.

- **Temporal smoothness** evaluates the consistency and fluidity of frame-to-frame transitions, and the naturalness of object movements within the video. Videos with high scores exhibit seamless transitions, smooth movements, and no noticeable inconsistencies, creating a natural and immersive viewing experience. Low scores denote irregular or abrupt frame changes and disjointed object movements, which detract from the overall fluidity. For detailed criteria, refer to Figure 15.
- **Dynamic degree** assesses the range and expressiveness of motion within the video. High-scoring videos display diverse, realistic, and natural movements of objects, animals, or humans, contributing to a vivid and engaging experience. Lower scores indicate limited motion or unnatural dynamics. This dimension highlights the importance of motion diversity and realism in engaging content. For detailed criteria, refer to Figure 16.
- **Text-video correspondence** examines the alignment between the video content and its associated text prompt. Videos with high scores perfectly match the descriptions in the prompt, accurately reflecting all elements with high fidelity. These videos effectively translate textual information into visual content without omissions or mismatches. In contrast, videos with lower scores exhibit inconsistencies, missing elements, or mismatched content. For detailed criteria, refer to Figure 17.

Each of these four dimensions is supported by detailed examples, providing annotators with clear guidelines to perform evaluations. This systematic approach ensures accuracy and consistency in the annotation process, enabling a robust analysis of human preference and video quality.

## C.2. Annotation Interface

To ensure a comprehensive and efficient evaluation of video quality, we designed two custom annotation interfaces tailored for different assessment tasks: one for score annotation and the other for pair annotation. The score annotation interface, shown in Figure 8, is a manual evaluation platform developed using the Python tkinter package, designed to facilitate MOS assessments. To ensure uniformity and minimize resolution-related biases in video quality evaluation, all videos displayed in this interface are cropped to a spatial resolution of 512×512 pixels. The duration of the videos remains unaltered, preserving the full content described in the associated text prompts. Meanwhile, the pair annotation interface, illustrated in Figure 9, supports paired comparison assessments, where participants evaluate two videos side-by-side. This interface is designed to explore preference judgments across four key aspects, in-

cluding: static Quality, temporal Smoothness, dynamic Degree, and text-Video Correspondence. In each comparison, participants are shown two videos, labeled "A" and "B," and are required to select their preferred video for each aspect. The interface ensures an unbiased evaluation environment by clearly distinguishing between the two videos while allowing side-by-side playback. Participants can replay either video as needed before making their selection. The evaluation process emphasizes subjective preferences while offering a structured approach to gather comparative insights across multiple dimensions. Navigation options, such as "Replay," "Next," and "Save," streamline the workflow, enabling efficient annotation

## C.3. Annotation Management

To ensure ethical compliance and the quality of annotations, we implemented a comprehensive process for the AIGVQA-DB dataset. All participants were fully informed about the experiment's purpose, tasks, and ethical considerations. Each participant signed an informed consent agreement, granting permission for their subjective ratings to be used exclusively for non-commercial research purposes. The dataset, consisting of 36,576 AI-generated videos (AIGVs) and their associated prompts, is publicly released under the CC BY 4.0 license. We ensured the exclusion of all inappropriate or NSFW content (textual or visual) through a rigorous manual review during the video generation stage. The annotation was divided into two key components: paired comparison annotation and MOS annotation, each designed to evaluate videos across four dimensions, including: static quality, temporal smoothness, dynamic degree, and text-video correspondence. For the paired comparisons, 30,000 video pairs were evaluated by a total of 100 participants. Each pair was assessed by three participants, and the final result for each pair was determined by majority voting. In cases of discrepancies, the average opinions of the three participants were calculated to resolve the tie. This approach ensured a balanced and fair evaluation of preferences between video pairs. The MOS annotation task involved 20 participants to rate all videos in the MOS subset individually. Participants scored each video on a 0-5 Likert scale across the four evaluation dimensions. This granular scoring provided a comprehensive dataset for analyzing human preferences and video quality.

Before participating in the annotation tasks, all participants underwent a rigorous training process. They were provided with detailed instructions, multiple standard examples (Figures 14-17), and step-by-step guidance on the annotation criteria. A pre-test was conducted to evaluate participants' understanding of the criteria and their agreement with standard examples. Those who did not meet the required accuracy were excluded from further participation. During the experiment, all evaluations were conducted in a



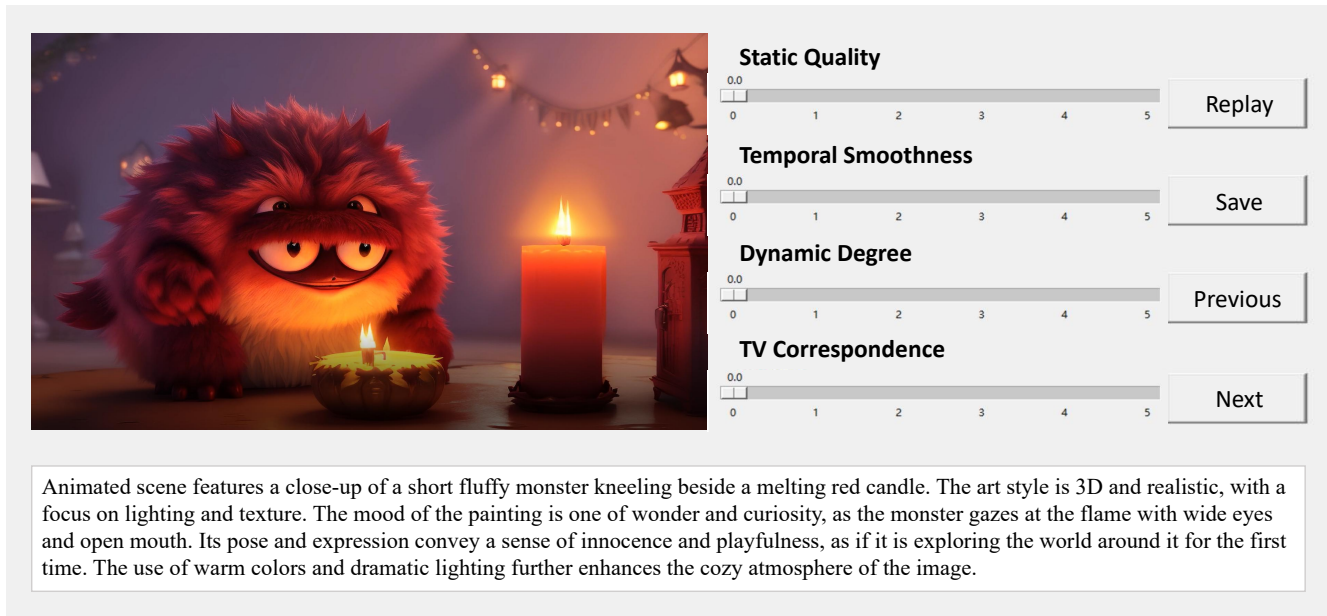


Figure 8. An example of the rating assessment interface for human evaluation. The subjects are instructed to rate four dimensions of AI-generated videos, i.e., static quality, temporal smoothness, dynamic degree, and text-video correspondence, based on the given video and its prompt.

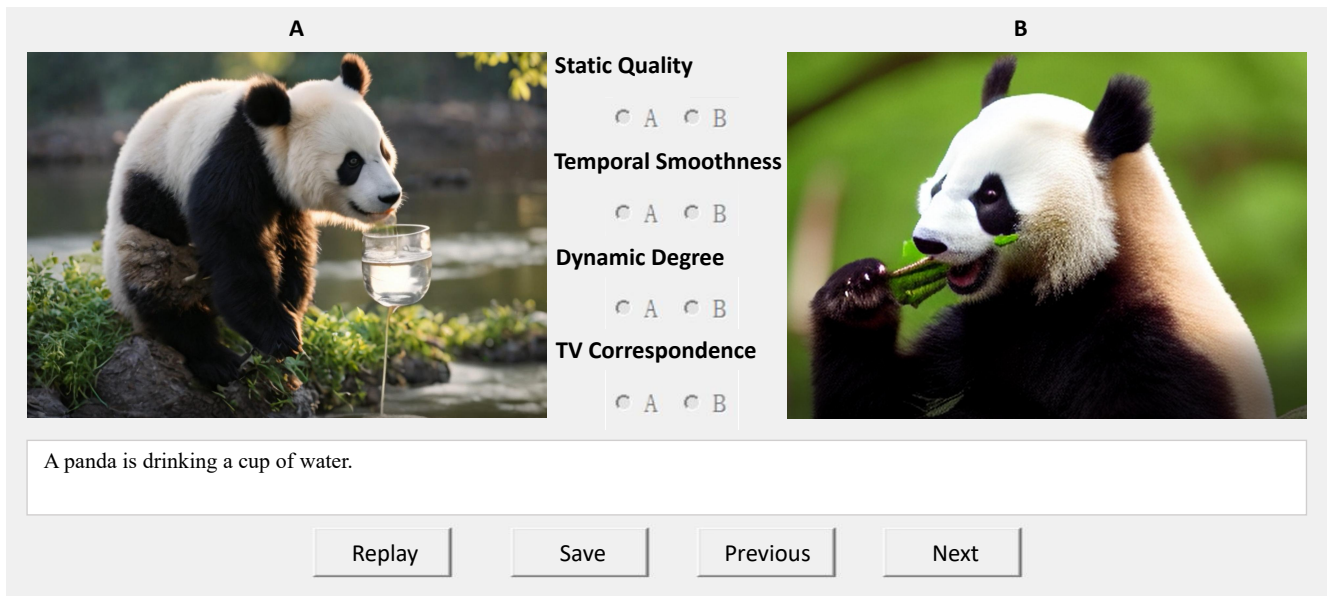


Figure 9. An example of the pair comparison assessment interface for human evaluation. The subjects are instructed to choose which AI-generated video is better among the video pairs, considering four dimensions respectively, i.e., static quality, temporal smoothness, dynamic degree, and text-video correspondence.

controlled laboratory environment with normal indoor lighting. Participants were seated at a comfortable viewing distance of approximately 60 cm from the screen. To further reduce potential biases, videos from different models were alternately presented in the both MOS and pair comparison

tasks. Although individual preferences may vary, the use of detailed explanations and standardized annotation criteria ensured a high level of agreement across participants. This consensus was particularly evident in pair annotations, where majority voting captured group preferences effec-

tively. The documentation of the entire annotation process served as a reference and training standard, ensuring consistency and reliability across all evaluations. This rigorous annotation management strategy makes AIGVQA-DB a robust and ethically sound resource for advancing research in video quality assessment.

## D. More Details of AIGVQA-DB

### D.1. Detailed Information of the Subsets

**Construction of the MOS subset.** The MOS subset is specifically designed to evaluate the perceptual quality of videos generated by T2V models, offering a comprehensive benchmark for subjective evaluation. This subset incorporates contributions from 12 generative models in the database, encompassing a broad spectrum of temporal and spatial attributes to ensure diversity. To construct this subset, we initially sourced 48 high-quality videos and their corresponding textual prompts from the Sora platform [7]. These prompts were then used to generate additional videos utilizing 11 other generative models, resulting in a total of 576 videos (48 prompts  $\times$  12 generative models). This approach ensured the inclusion of a wide range of visual styles and generative qualities. The dataset spans significant variations in frame count, frame rate (FPS), and resolution, ranging from the compact 256 $\times$ 256 outputs of VideoFusion [43] at 8 FPS to the high-definition 1920 $\times$ 1080 outputs of Sora at 30 FPS. Such diversity in video attributes allows for a robust analysis of generative models under different visual and temporal conditions. Each video in the MOS subset is evaluated by 20 annotators across four dimensions: Static Quality, Temporal Smoothness, Dynamic Degree, and Text-Video Correspondence. This rigorous evaluation process results in 46,080 individual ratings (4 dimensions  $\times$  576 videos  $\times$  20 annotators). The annotators, equipped with detailed training and examples, provide subjective scores on a 0-5 Likert scale, ensuring consistency and reliability in their assessments. By including videos with diverse visual properties, the MOS subset provides a robust foundation for subjective evaluation tasks, enabling researchers to compare T2V models based on the perceptual quality of AIGVs.

**Construction of the Pair comparison subset.** To enable detailed comparative analysis, we construct the pair comparison subset. This subset is built based on 1,000 carefully curated textual prompts, including a wide range of scenarios, themes, and levels of complexity. These prompts ensure diversity in content and provide a robust basis for assessing the performance of generative models across various contexts. We use 12 generative models, including 8 open-source models such as Hotshot-XL [1] and Floor33 [2], and 4 closed-source models, such as Gen-2 [4] and MoonValley [5]. For each prompt, open-source models generate four distinct videos, capturing variations in their generative out-

puts and showcasing intra-model diversity. Closed-source models, due to access constraints, produce one video per prompt. This comprehensive approach results in a dataset of 36,000 videos (1,000 prompts  $\times$  (8 open-source models  $\times$  4 videos + 4 closed-source models  $\times$  1 video)). The videos in this subset exhibit a wide range of resolutions and frame counts, from the lower-resolution 256 $\times$ 256 outputs of LVDM [19] to the high-definition 1920 $\times$ 1080 videos from MorphStudio [6]. Each video pair is evaluated by three annotators, who provide individual ratings for all four dimensions. These ratings are aggregated to determine the final result for each dimension, with majority voting or averaged scores used to resolve any disagreements. This process results in 360,000 (4  $\times$  30,000  $\times$  3) ratings, ensuring a rigorous and nuanced analysis of model performance. The pair-comparison subset allows for head-to-head comparisons of generative models, and provides valuable insights into the strengths and weaknesses of different models, offering researchers a robust foundation for comparative studies.

### D.2. More Result Analysis

We analyze the subjective pair ratings by calculating the win rates of different generation models across different categories, revealing strengths and weaknesses from four different dimensions. For the evaluation of spatial content categories, as shown in Figure 10(a), models like Genmo [3] perform exceptionally well in generating realistic representations of people, animals, and vehicles showcasing their strong attention to detail and visual fidelity. MorphStudio [6] consistently leads in producing high-quality outputs for scenery and natural objects, excelling in generating visually appealing and immersive natural environments. Additionally, StableVideoDiffusion [9] demonstrates notable strength in creating illustrations, highlighting its flexibility in handling stylized and artistic content. Conversely, LVDM [19] and VideoFusion [43] lag in these categories, struggling with resolution and detail preservation. For the evaluation of temporal content categories, as shown in Figure 10(b), MorphStudio [6] excels in handling kinetic motions, fluid motions, actions, and scenarios with light changes, making its outputs maintain high temporal smoothness and text-video correspondence. However, models like Text2Video-Zero [26] occasionally produce abrupt transitions, and Tune-A-Video [72] shows limitations in maintaining temporal smoothness under complex motion conditions. For the evaluation of attribute control categories, as shown in Figure 10(c), Genmo [3] performs well in maintaining appropriate quantities of objects. Floor33 [2] and VideoCrafter [10] display superior performance in the logical sequence of events. In contrast, StableVideoDiffusion [9] encounters challenges in event order. Its generative process involves first creating static images and subsequently animating them to produce video sequences. The

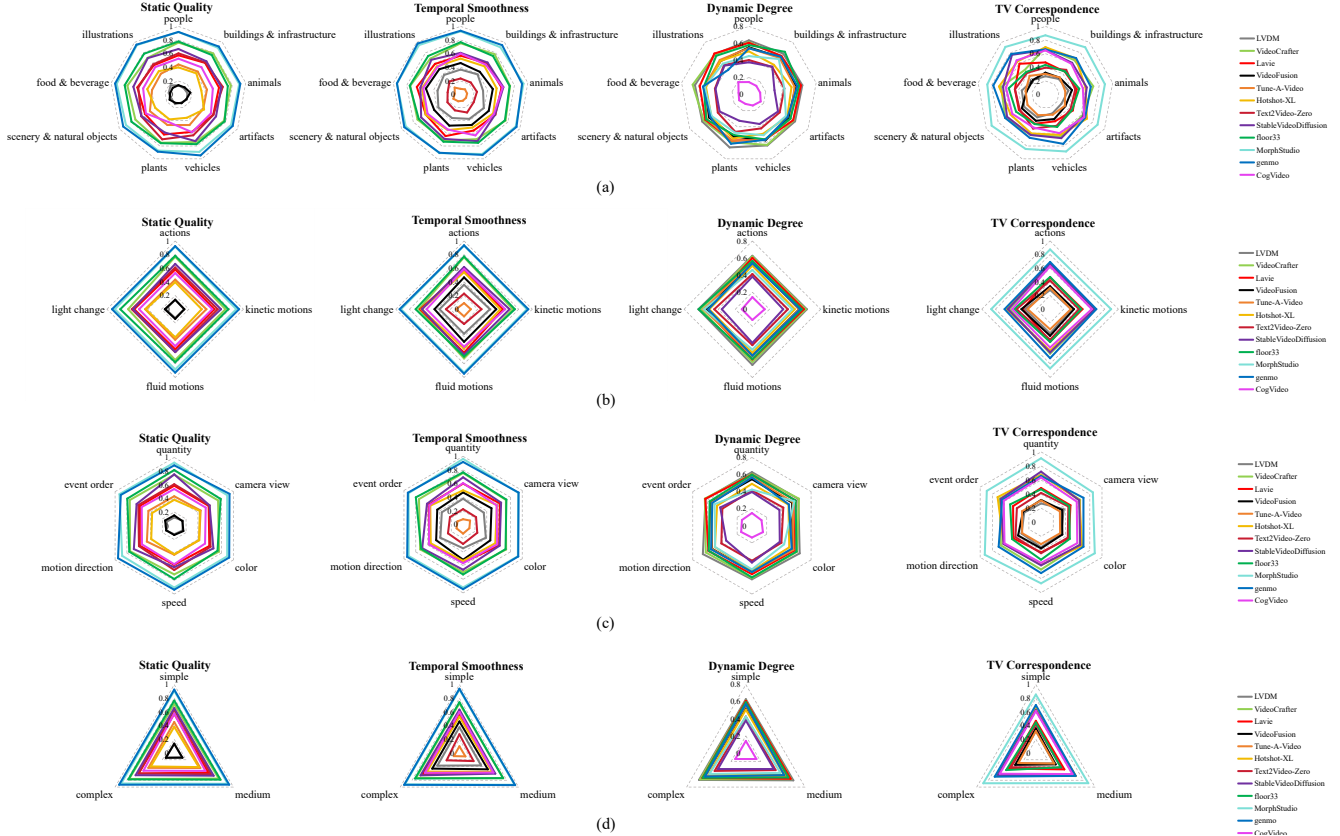


Figure 10. Comparison of averaged win rates of different generation models across different categories. (a) Results across spatial major contents. (b) Results across temporal major contents. (c) Results across dynamic degrees. (d) Results across text-to-video correspondence.

static-to-dynamic generation pipeline introduces discrepancies in temporal alignment, making it difficult to ensure that actions unfold in a logically consistent manner. For the evaluation of prompt complexity categories, as shown in Figure 10(d), most models demonstrate competence in handling prompts of different complexity, likely due to shared architectures like diffusion-based systems, with common strengths and limitations in handling complex prompts.

## E. Details of Loss Function

The training process for AIGV-Assessor is divided into three progressive stages, each utilizing a specific loss function to target distinct objectives: language loss for aligning visual and language features, L1 loss for generating accurate quality scores, and cross-entropy loss for robust pairwise video quality comparisons.

**(1) Aligning visual and language features with language loss.** In the first stage, spatial and temporal projectors are trained to align visual and language features using the language loss. This involves ensuring that the visual tokens extracted from the vision encoder correspond effectively to the language representations from the LLM. The language loss, calculated using a cross-entropy function, measures

the model’s ability to predict the correct token given the prior context:

$$\mathcal{L}_{\text{language}} = -\frac{1}{N} \sum_{i=1}^N \log P(y_{\text{label}} | y_{\text{pred}}) \quad (1)$$

where  $P(y_{\text{label}} | y_{\text{pred}})$  represents the probability assigned to the correct token  $y_{\text{label}}$  by the model,  $y_{\text{pred}}$  is the predicted token, and  $N$  is the total number of tokens. By minimizing this loss, the model learns to generate coherent textual descriptions of video content, laying the foundation for subsequent stages.

**(2) Refining quality scoring with L1 loss.** Once the model can produce coherent descriptions of video content, the focus shifts to fine-tuning the quality regression module to output stable and precise numerical quality scores. The quality regression module takes the aligned visual tokens as input and predicts a quality score that reflects the overall video quality. Using the AIGVQA-DB, which contains human-annotated MOS for each video, the model is trained to align its predictions with human ratings. The training objective minimizes the difference between the predicted quality score  $Q_{\text{predict}}$  and the ground-truth MOS  $Q_{\text{label}}$  using

the L1 loss function:

$$\mathcal{L}_{\text{MOS}} = \frac{1}{N} \sum_{i=1}^N |Q_{\text{predict}}(i) - Q_{\text{label}}(i)| \quad (2)$$

where  $Q_{\text{predict}}(i)$  is the score predicted by the regressor  $i$  and  $Q_{\text{label}}(i)$  is the corresponding ground-truth MOS derived from subjective experiments, and  $N$  is the number of videos in the batch. This loss function ensures that the predicted scores remain consistent with human evaluations, enabling the model to accurately assess the quality of AI-generated videos in numerical form.

**(3) Enhancing pairwise comparisons with cross-entropy Loss.** The third stage incorporates the AIGVQA-DB subset into the training pipeline. This dataset contains human annotations for pairwise video comparisons, where two videos are evaluated, and the superior one is selected based on quality. Pairwise training helps the model learn relative quality distinctions, enabling it to compare videos effectively. The objective in this stage is to maximize the probability that the model predicts a higher score for the better video in a pair. The pairwise comparison loss is calculated by comparing the predicted scores for a video pair, which are processed through an LPIPS network to judge which video is better. This predicted logit is then compared with the ground-truth logit labels (0 or 1) using the cross-entropy loss. The label 0 indicates that video2 is better, and 1 indicates that video1 is better. The order of the pair (which video is considered as video1 or video2) is random, but the logit label always corresponds correctly to the better video.

$$\mathcal{L}_{\text{Pairs}} = -\frac{1}{N} \sum_{i=1}^N [y_{\text{label}}(i) \log y_{\text{pred}}(i) + (1 - y_{\text{label}}(i)) \log(1 - y_{\text{pred}}(i))] \quad (3)$$

where  $y_{\text{pred}}$  is the logit predicted by the network for the video pair,  $y_{\text{label}}$  is the ground-truth label for the video pair (0 for video2 better, 1 for video1 better), and  $N$  is the number of videos in the batch. This function encourages the model to predict the better video in a pair, reinforcing its ability to make accurate comparisons. By incorporating the pairwise data into training, the model not only learns to provide accurate quality scores but also becomes proficient in comparing videos and selecting the superior one. This enhances its utility in real-world applications, where users often need to compare the quality of multiple videos directly.

## F. Implementation Details

### F.1. Detailed Information of Evaluation Criteria

We adopt the widely used metrics in VQA literature [13, 49]: Spearman rank-order correlation coefficient (SRCC), Pearson linear correlation coefficient (PLCC), and

Kendall’s Rank Correlation Coefficient (KRCC) as our evaluation criteria. SRCC quantifies the extent to which the ranks of two variables are related, which ranges from -1 to 1. Given  $N$  action videos, SRCC is computed as:

$$\text{SRCC} = 1 - \frac{6 \sum_{n=1}^N (v_n - p_n)^2}{N(N^2 - 1)}, \quad (4)$$

where  $v_n$  and  $p_n$  denote the rank of the ground truth  $y_n$  and the rank of predicted score  $\hat{y}_n$  respectively. The higher the SRCC, the higher the monotonic correlation between ground truth and predicted score. Similarly, PLCC measures the linear correlation between predicted scores and ground truth scores, which can be formulated as:

$$\text{PLCC} = \frac{\sum_{n=1}^N (y_n - \bar{y})(\hat{y}_n - \bar{\hat{y}})}{\sqrt{\sum_{n=1}^N (y_n - \bar{y})^2} \sqrt{\sum_{n=1}^N (\hat{y}_n - \bar{\hat{y}})^2}}, \quad (5)$$

where  $\bar{y}$  and  $\bar{\hat{y}}$  are the mean of ground truth and predicted score respectively. We also adopt the Kendall Rank Correlation Coefficient (KRCC) as an evaluation metric, which measures the ordinal association between two variables. For a pair of ranks  $(v_i, p_i)$  and  $(v_j, p_j)$ , the pair is concordant if:

$$(v_i - v_j)(p_i - p_j) > 0, \quad (6)$$

and discordant if  $< 0$ . Given  $N$  AIGVs, KRCC is computed as:

$$\text{KRCC} = \frac{C - D}{\frac{1}{2}N(N - 1)}, \quad (7)$$

where  $C$  and  $D$  denote the number of concordant and discordant pairs, respectively.

### F.2. Detailed Information of Evaluation Algorithms

**V-Dynamic** [24] and **V-Smoothness** [24] are proposed in VBench [24]. We directly used the respective implementation code in VBench [24] without specific changes.

**CLIPScore** [20] is an image captioning metric, which is widely used to evaluate T2I/T2V models. It passes both the image and the candidate caption through their respective feature extractors, then computing the cosine similarity between the text and image embeddings. **BLIPScore** [36] replace CLIP with BLIP [36] to compute the cosine similarity. **ImageReward** uses BLIP [36] as the backbone, and uses an MLP to generate a scalar for preference comparison. **AestheticScore** is given by an aesthetic predictor introduced by LAION [54].

**VSFA** [34] is an objective no-reference video quality assessment method by integrating two eminent effects of the human visual system, namely, content-dependency and temporal-memory effects into a deep neural network. We directly used the official code without specific changes.

**BVQA** [32] leverages the transferred knowledge from IQA databases with authentic distortions and large-scale action

recognition with rich motion patterns for better video representation. We used the officially pre-trained model under mixed-database settings and finetuned it on our AIGVQA-DB for evaluation.

**SimpleVQA** [57] adopts an end-to-end spatial feature extraction network to directly learn the quality-aware spatial feature representation from raw pixels of the video frames and extract the motion features to measure the temporal-related distortions. A pre-trained SlowFast model is used to extract motion features. We used the officially pre-trained model and finetuned it on our AIGVQA-DB for evaluation.

**FAST-VQA** [69] proposes a grid mini-patch sampling strategy, which allows consideration of local quality by sampling patches at their raw resolution and covers global quality with contextual relations via mini-patches sampled in uniform grids. It overcomes the high computational costs when evaluating high-resolution videos. We used the officially released FAST-VQA-B model and finetuned it on our AIGVQA-DB.

**DOVER** [70] is a disentangled objective video quality evaluator that learns the quality of videos based on technical and aesthetic perspectives. We used the officially pre-trained model and finetuned it on our AIGVQA-DB.

**Q-Align** [71] is a human-emulating syllabus designed to train large multimodal models for visual scoring tasks. It mimics the process of training human annotators by converting MOS into five text-defined rating levels. We used the officially pre-trained model and finetuned it on our AIGVQA-DB.

Table 10. Examples of prompts and their corresponding categorizations in AIGVQA-DB.

Prompts	Spatial major content	Temporal major content	Attribute control	Complexity	Source
"A person is running backwards."	people	actions, kinetic motions	motion direction	simple	FETV [42]
"A plane is flying backwards."	vehicles	kinetic motions	motion direction	simple	FETV [42]
"A blue horse is running in the field."	animals	actions, kinetic motions	color	simple	FETV [42]
"A green shark is swimming under the water."	animals	fluid motions, actions, kinetic motions	color	simple	FETV [42]
"A leave is flying towards the tree from the ground."	plants	kinetic motions	motion direction	medium	FETV [42]
"The flowers first wilt and then bloom again."	plants	fluid motions	event order	simple	FETV [42]
"The sun sets on the horizon and then immediately rises again."	scenery and natural objects	kinetic motions	event order	medium	FETV [42]
"A person pours a cup of coffee from a bottle and then pours the coffee back to the bottle."	people, food and beverage	actions, fluid motions	event order	complex	FETV [42]
"The three singers are dancing in swim suits."	people	actions	quantity	simple	InternVid [67]
"a bearded man nods and blows kisses."	people	actions	event order	simple	InternVid [67]
"A dog are flipping and riding a skateboard."	animals	actions	null	simple	InternVid [67]
"A white puppy plays with a slice of lime"	animals, food and beverage	kinetic motions	color	medium	InternVid [67]
"Rain is falling on a black umbrella."	plants, scenery and natural object	fluid motions	color	simple	InternVid [67]
"Two cars are racing on a track."	vehicles	kinetic motions	quantity	simple	InternVid [67]
"Two very handsome boys are singing on the stage."	people	actions	quantity	medium	InternVid [67]
"Two girls are standing in the ocean when they become frightened of something in the water."	people	actions	quantity, event order	complex	InternVid [67]
"An arial view of animals running"	animals	actions, kinetic motions	camera view	simple	MSRVTT [75]
"Overhead view as pingpong players compete on the table"	people	actions, kinetic motions	camera view	medium	MSRVTT [75]
"There is a orange color fish floating in the water"	animals	fluid motions	color	medium	MSRVTT [75]
"Some blue water in a pool is rippling around"	scenery and natural objects	fluid motions	color	medium	MSRVTT [75]
"A red sport car is driving very fast"	vehicles	kinetic motions	color, speed	medium	MSRVTT [75]
"Four friends are driving in the car"	scenery and natural objects	fluid motions	color	medium	MSRVTT [75]
"Smoke is coming out of a mountain"	scenery and natural objects	fluid motions	motion direction	simple	MSRVTT [75]
"Satellite view of moon we can also see sunlight but surface is not smooth"	scenery and natural objects	light change	camera view	complex	MSRVTT [75]
"Smoke billows from the factory chimney."	vehicles, buildings and infrastructure	fluid motions	color	simple	Handwritten
"Leaves flutter from the trees in the gusty wind."	plants	kinetic motions	motion direction	medium	Handwritten
"The crimson hues painted the horizon during the beach sunset."	scenery and natural objects	light change	color	medium	Handwritten
"The static view of a solar eclipse revealed nature's cosmic spectacle."	scenery and natural objects	light change	camera view	medium	Handwritten
"A hiker reaches the summit and then admires the breathtaking view."	people	actions	event order	medium	Handwritten
"Vinegar drizzling onto a salad, filmed in intricate detail."	food and beverage	fluid motions	camera view	medium	Handwritten
"An egg cracking open and being whisked vigorously in slow motion."	food and beverage	kinetic motions	speed	medium	Handwritten
"The coastline transformed into a canvas of fiery colors during the beach sunset."	scenery and natural objects	light change	color	complex	Handwritten
"Two men playing musical instruments in a city square."	people, artifacts	kinetic motions	quantity	medium	TGIF [37]
"The bridge of a river being viewed from a cable."	scenery and natural object	kinetic motions	camera view	medium	TGIF [37]
"A view from inside of a bus showing snow"	vehicles, scenery and natural object	kinetic motions	camera view	medium	TGIF [37]
"Some large metal barrels on a train track."	vehicles, artifacts	actions	quantity	simple	TGIF [37]
"A person reaching into a dish of beef and vegetables."	people, food and beverage	actions	quantity	medium	TGIF [37]
"A man wearing a green jacket is fixing a solar panel."	people	actions	color	medium	TGIF [37]
"A green toy chamelon eating a cookie."	animals, food and beverage	kinetic motions	color	simple	TGIF [37]
"Two people sit on a table with headphones on"	people	actions	quantity	medium	TGIF [37]
"A screenshot of the dashboard of a korean language software"	illustrations	actions	camera view	medium	TGIF [37]
"A woman's tight pants with two photos, one showing her wearing the pants and the other showing her with a shirt."	people, artifacts	actions	quantity	complex	TGIF [37]
"Background - sunset landscape beach."	scenery and natural object	light change	null	simple	WebVid [8]
"The musician plays the guitar. close up."	people, artifacts	actions	camera view	simple	WebVid [8]
"Background - sunset landscape beach."	scenery and natural object	light change	null	simple	WebVid [8]
"Background - sunset landscape beach."	scenery and natural object	light change	null	simple	WebVid [8]
"Background - sunset landscape beach."	scenery and natural object	light change	null	simple	WebVid [8]
"Attractive young woman silhouette dancing outdoors on a sunset with sun shining bright behind her on a horizon. slow motion."	people, scenery and natural object	actions, light change	speed	complex	WebVid [8]
"Night landscape timelapse with colorful milky way. starry sky with tropical palms on the island. milky way timelapse over palms."	plants, scenery and natural object	light change	speed	complex	WebVid [8]
"A blue wave of fire grows into a large flame and bright sparks on a shiny surface. closeup. slow motion, high speed camera."	scenery and natural object	fluid motions, light change	camera view, color, speed	complex	WebVid [8]
"Silhouette of happy mom dad and baby at sunset in a field with wheat. farmer and family on the field. a child with parents plays in the wheat. the concept of family relationships."	people, plants	actions, light change	null	complex	WebVid [8]
"Traditional chinese ink preparation. low angle dolly shot close up focus from brushes on ceramic stand to person hands in background preparing ink for calligraphy."	artifacts, people	actions	camera view	complex	WebVid [8]
"Beautiful growing network with economic indicators growing abstract seamless. looped 3d animation of moving numbers and lines. cyberspace flashing lights. business concept. 4k ultra hd 3840x2160."	illustrations	light change	camera view	complex	WebVid [8]

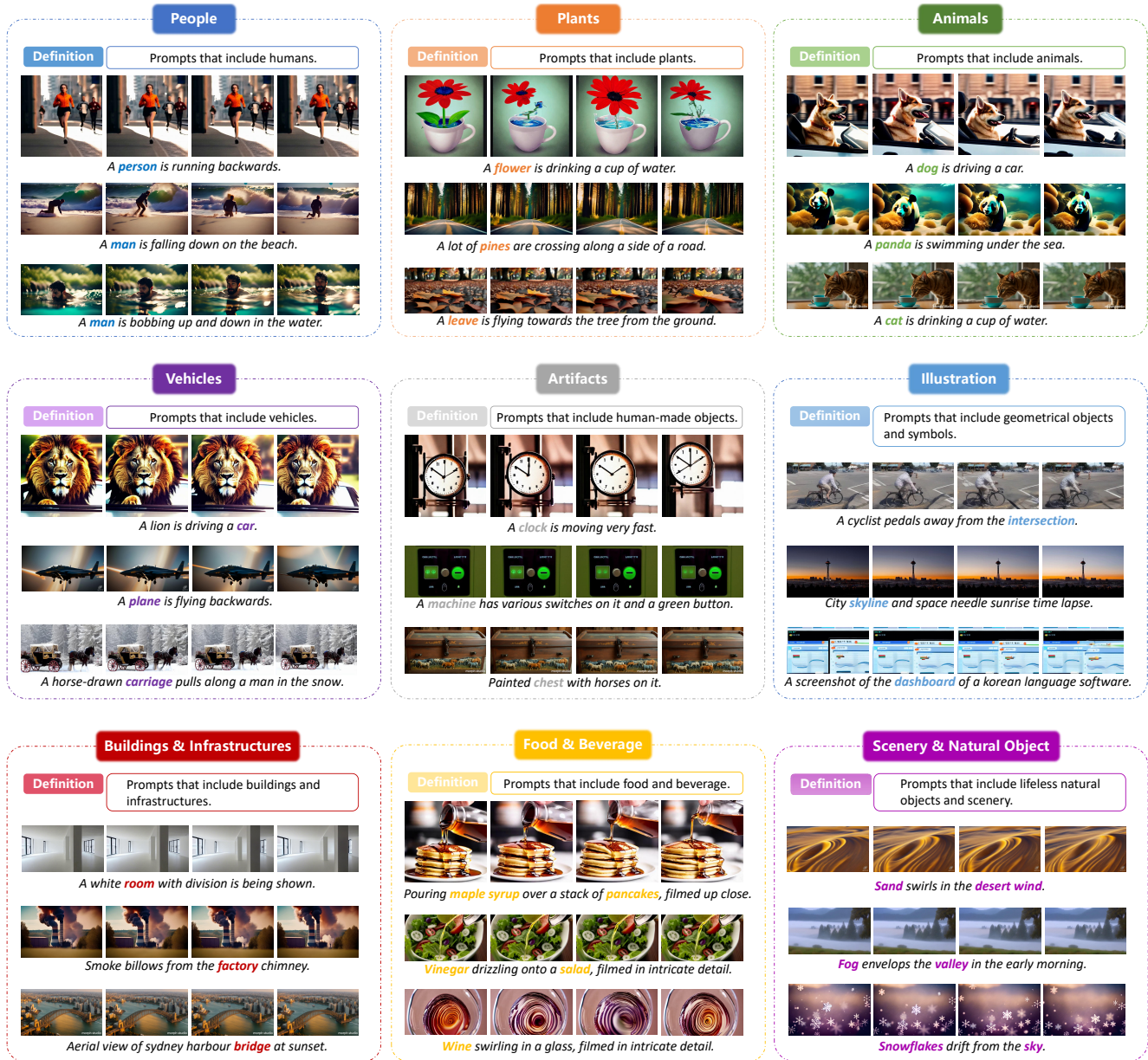


Figure 11. Descriptions and examples of the spatial major contents.

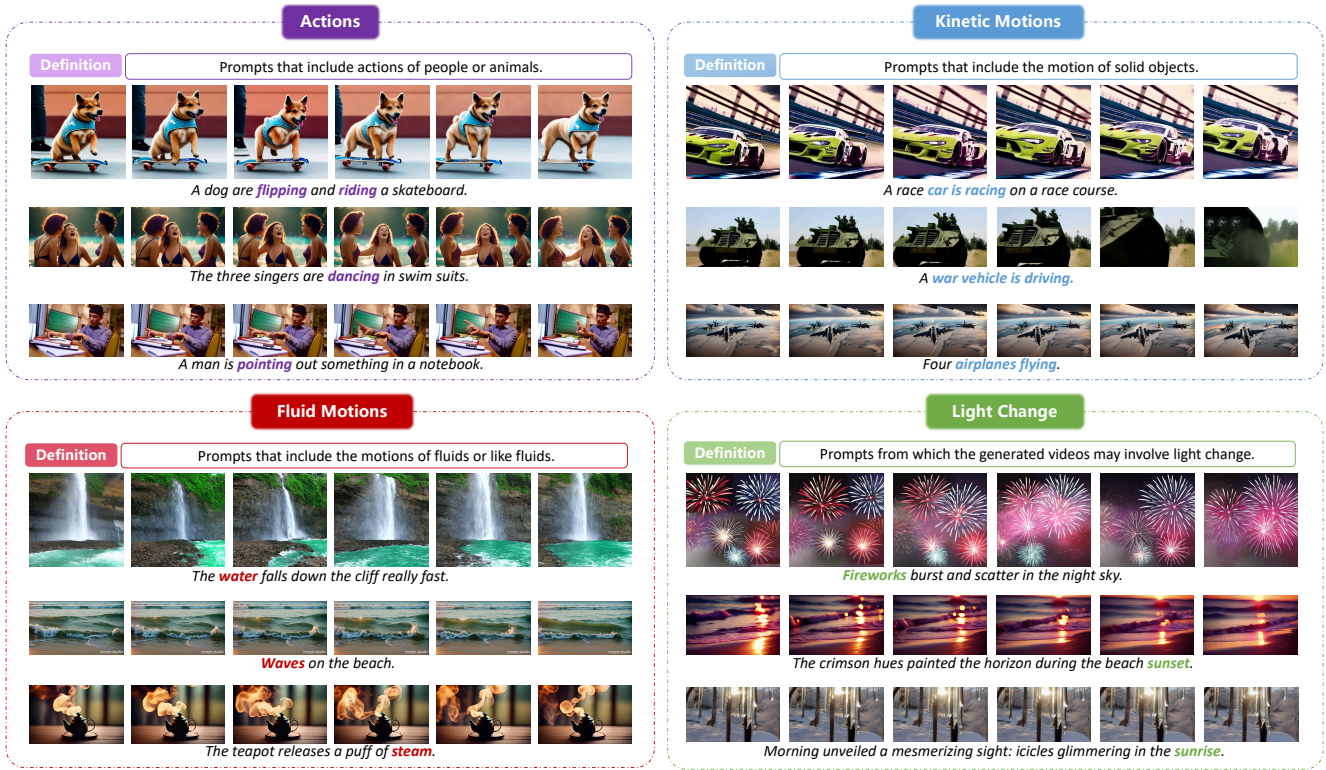


Figure 12. Descriptions and examples of the temporal major contents.

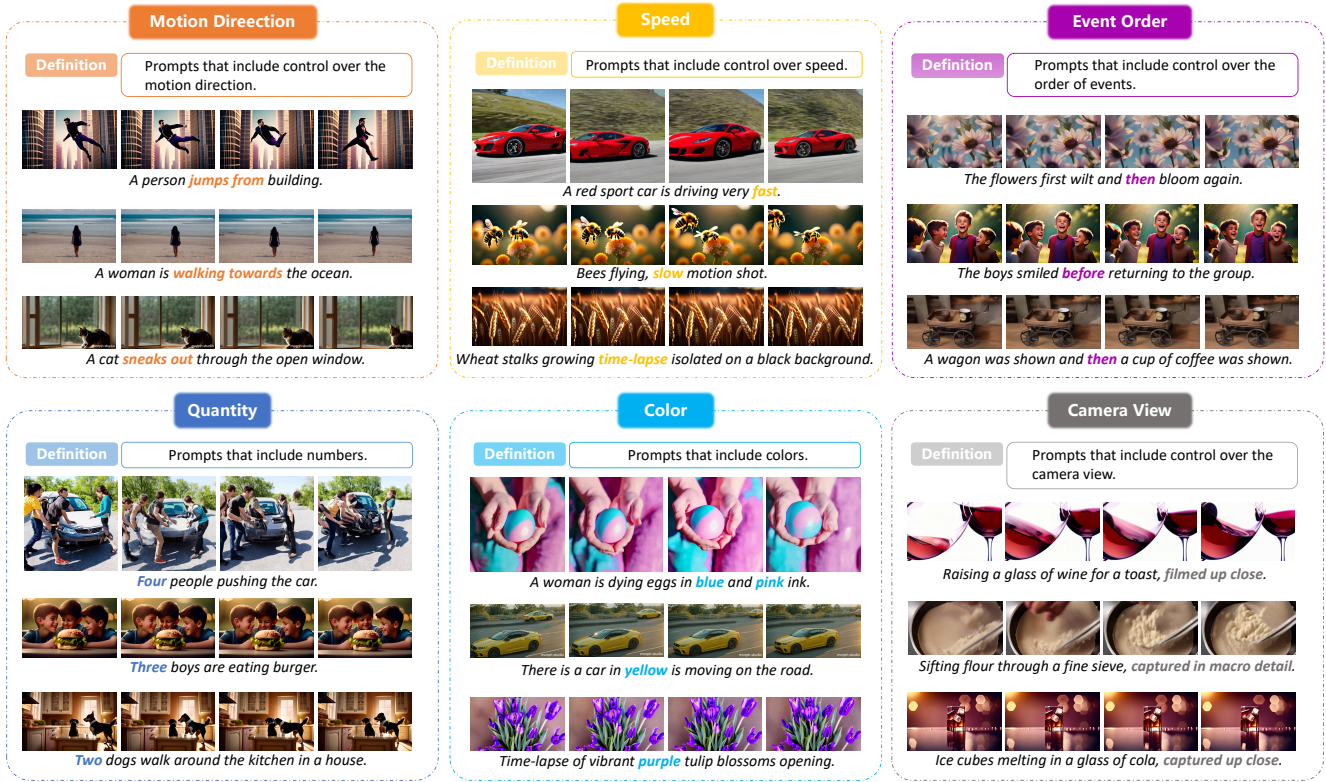
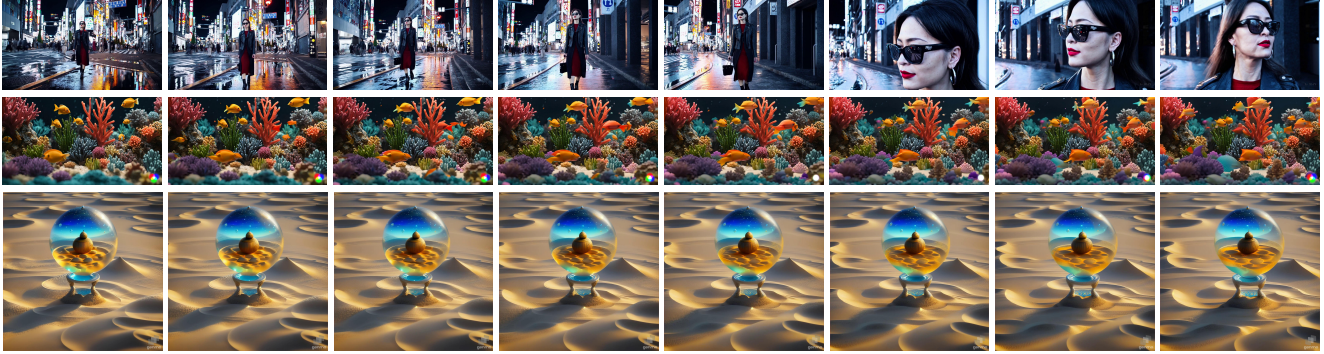


Figure 13. Descriptions and examples of the attribute control.



Static quality **4-5 (Excellent)**: The video content is exceptionally clear, and natural, with vivid and well-balanced colors. All details are flawlessly presented, resulting in a high-quality, immersive, and visually striking experience.



Static quality **3-4 (Good)**: The video content is reasonably clear and natural, with well-preserved details and fairly vibrant colors. The overall quality is satisfactory, offering a pleasant and visually appealing experience.



Static quality **2-3 (Fair)**: The video content shows slight blurriness or appears somewhat unnatural, with colors that are somewhat muted or inconsistent. The quality is acceptable but lacks sharpness, smoothness, or vibrant colors, making it less engaging or realistic.



Static quality **1-2 (Poor)**: The video content is noticeably blurry or unnatural, and the colors appear faded or washed out. While some details may still be identifiable, the lack of clarity and vibrancy results in a poor viewing experience.

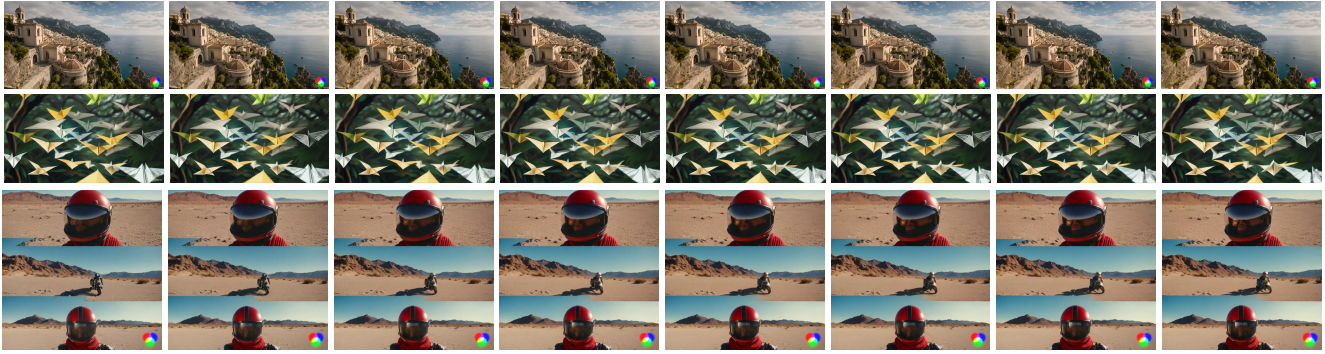


Static quality **0-1 (Bad)**: The video content extremely blurry or highly unnatural, with dull or distorted colors, making it difficult to discern details or recognize objects clearly.

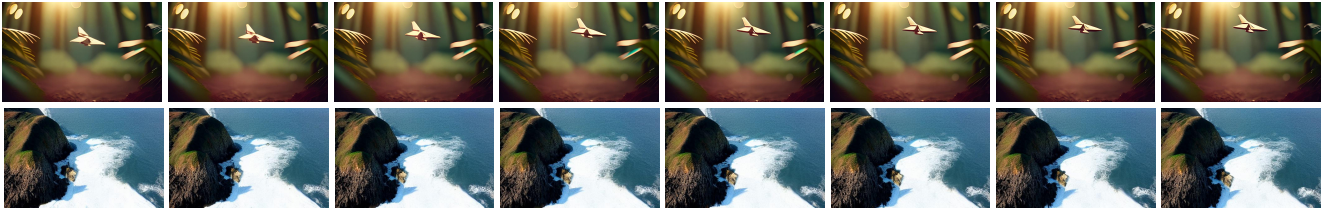


Figure 14. Instructions and examples for manual evaluation of **static quality**.

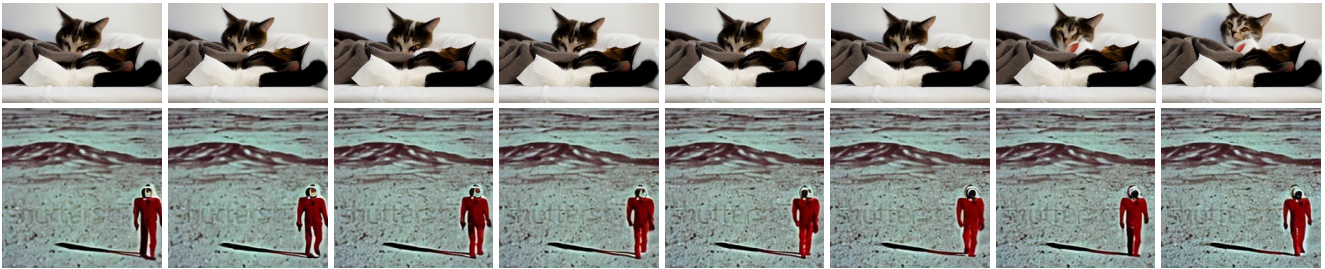
Temporal smoothness **4-5 (Excellent)**: The video exhibits perfectly smooth frame-to-frame transitions, with natural movements and no noticeable inconsistencies in objects or appearances. Object positions are fluid and realistic, creating an immersive and seamless viewing experience.



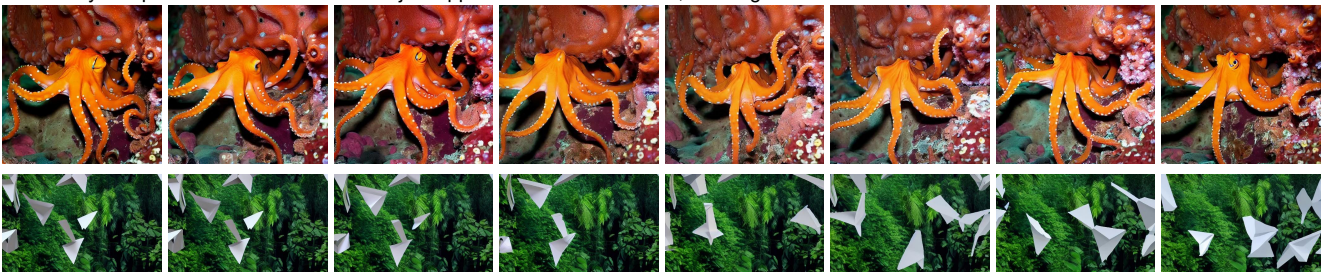
Temporal smoothness **3-4 (Good)**: Frame transitions are mostly smooth, with only rare and minor inconsistencies in object appearance or slight unnatural movements. Object positions and motions are generally well-aligned, and the video feels coherent and natural for the most part.



Temporal smoothness **2-3 (Fair)**: The frame-to-frame transitions are somewhat consistent, but minor unnatural movements, subtle object deformations, or occasional appearance inconsistencies may occur.



Temporal smoothness **1-2 (Poor)**: Frame transitions are notably rough, with visible unnatural movements or occasional jumps in object positions. There may be sporadic inconsistencies in object appearance or deformation, creating a sense of disconnection between frames.



Temporal smoothness **0-1 (Bad)**: The transitions between frames are highly inconsistent, with noticeable object position jumps, severe unnatural movements, or deformations. Inconsistent objects or appearances are frequent, making the video jarring and disjointed.

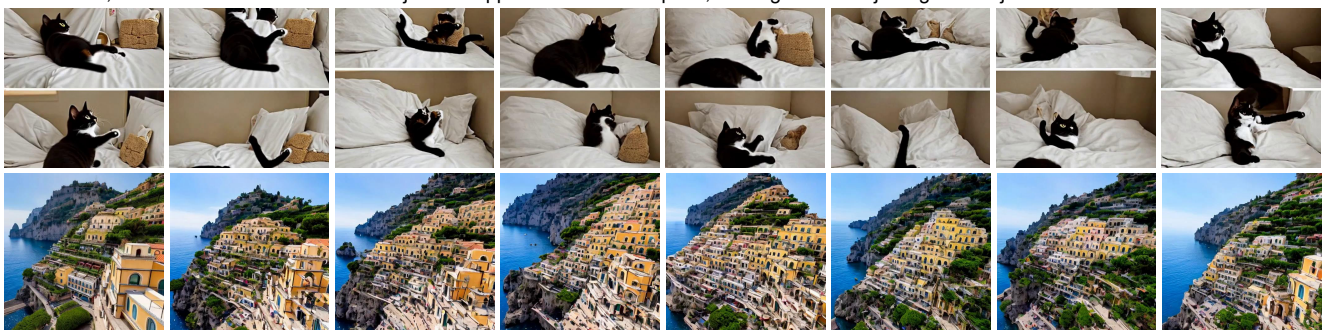
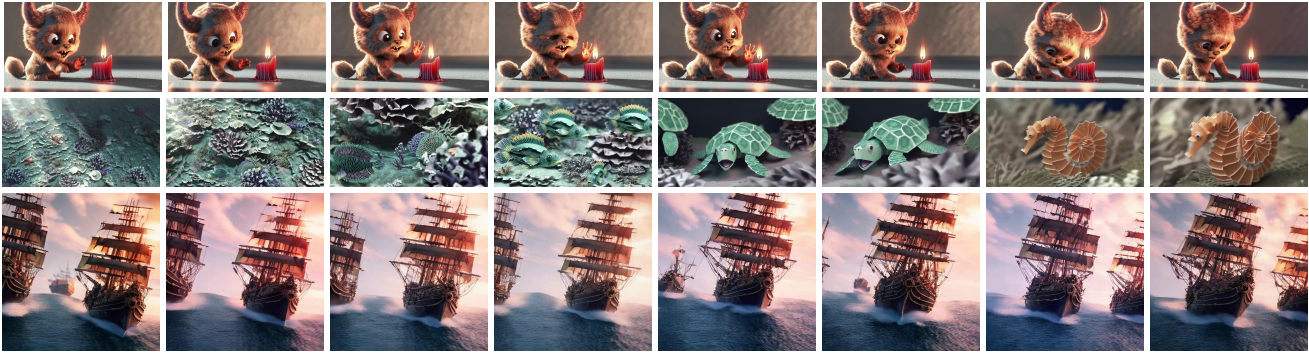


Figure 15. Instructions and examples for manual evaluation of **temporal smoothness**.

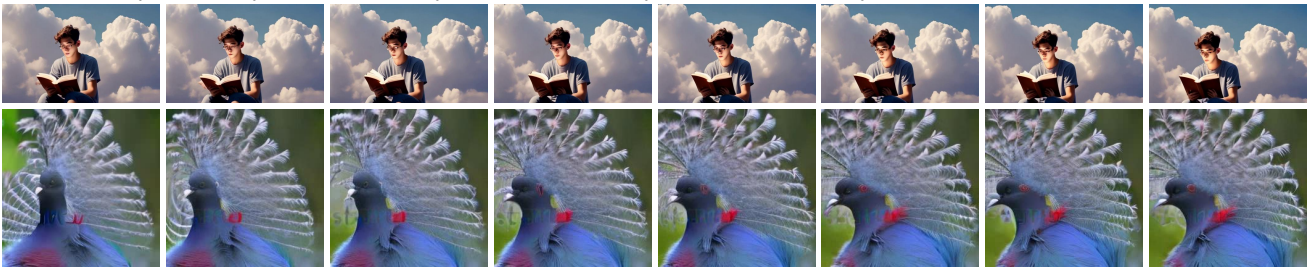
Dynamic degree **4-5 (Excellent)**: The video exhibits a highly dynamic degree of motion, with humans, animals, or objects moving across a wide range in a natural and expressive manner. The movements are diverse, creating a vivid and highly engaging visual experience.



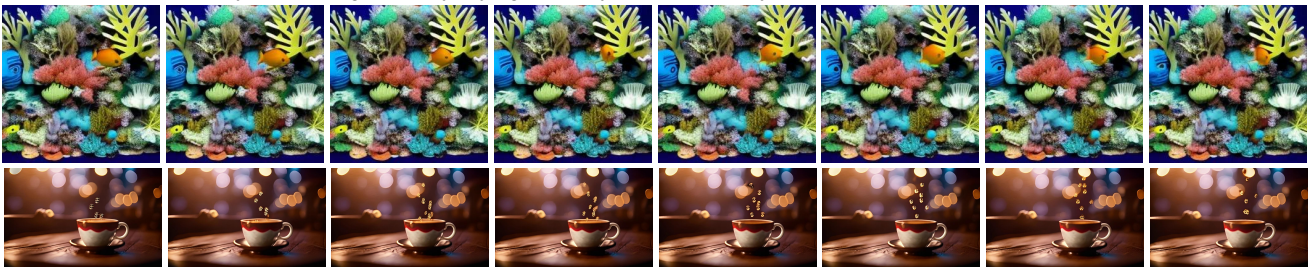
Dynamic degree **3-4 (Good)**: The video contains a broad range of motion, with humans, animals, or objects moving naturally. The movements are engaging and visually dynamic, with clear activity that maintains viewer interest.



Dynamic degree **2-3 (Fair)**: The video displays moderate motion, with humans, animals, or objects moving across a somewhat confined range. Movements may occasionally feel limited, but they are sufficient to convey a basic sense of activity.



Dynamic degree **1-2 (Poor)**: The video shows limited motion, with only small, repetitive, or localized movements. The range of motion is restricted, and the content feels overly static, failing to convey any significant dynamism or activity.

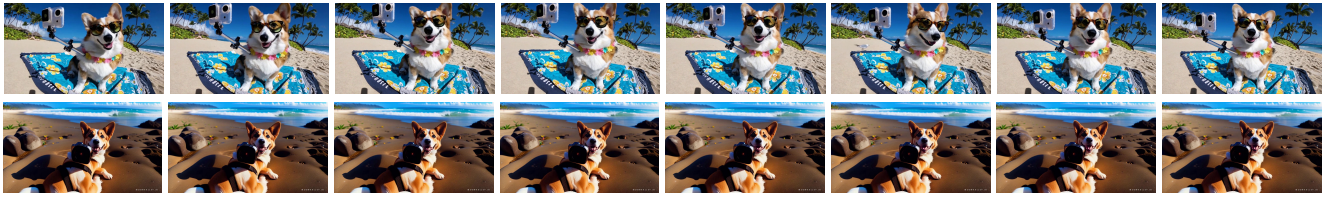


Dynamic degree **0-1 (Bad)**: The motion in the video is almost nonexistent, with minimal or no visible movement of humans, animals, or objects. The content appears static or lifeless, lacking any dynamic visual interest.



Figure 16. Instructions and examples for manual evaluation of **dynamic degree**.

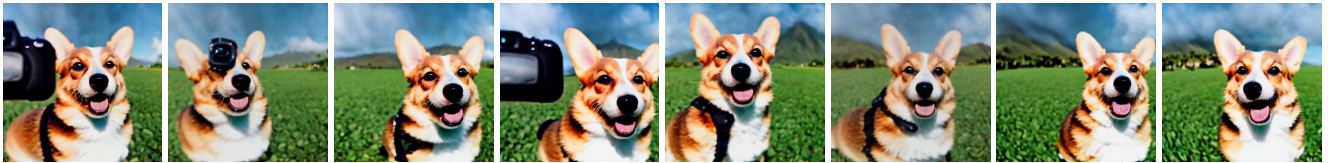
Text-video correspondence **4-5 (Excellent)**: The video content perfectly aligns with the prompt. All described elements are fully realized with high fidelity, leaving no noticeable differences or omissions. The video effectively and naturally captures the exact meaning and intent of the text.



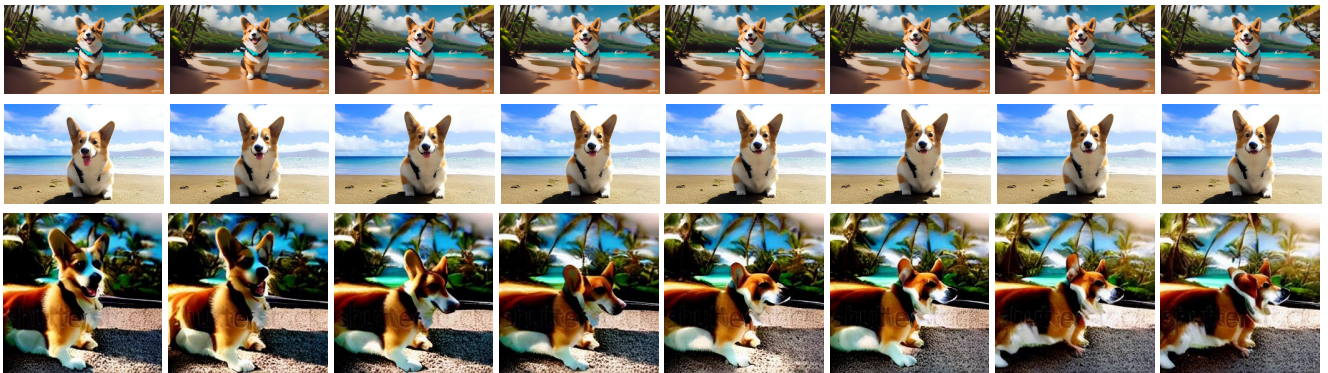
Text-video correspondence **3-4 (Good)**: The video closely matches the prompt, with most key elements represented accurately and in detail. There may be minor omissions or differences, but they do not detract significantly from the overall correspondence between the text and the video.



Text-video correspondence **2-3 (Fair)**: The video content partially aligns with the prompt. Core elements are present, but some details might be missing, incomplete, or slightly different. The overall correspondence is acceptable but lacks precision or completeness.



Text-video correspondence **1-2 (Poor)**: The video shows limited correspondence with the prompt. While some elements might loosely match, there are noticeable discrepancies, missing features, or incorrect interpretations of the text.



Text-video correspondence **0-1 (Bad)**: The video content is entirely inconsistent with the prompt. Key elements described in the prompt are either missing or incorrectly represented, resulting in a complete lack of correspondence to the text.

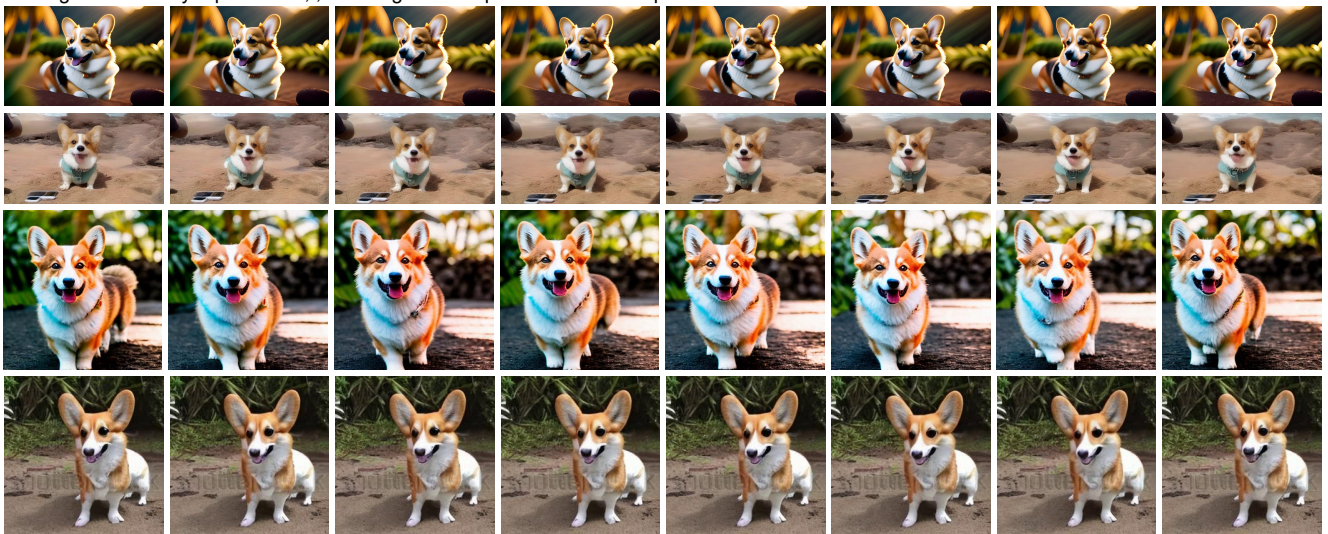


Figure 17. Instructions and examples for manual evaluation of **text-video correspondence**. The example videos are of the same prompt “A corgi vlogging itself in tropical Maui.”